To the Graduate Council:

I am submitting herewith a thesis written by Julie Ann Darnell entitled "Prediction of Flame Blowoff Limits for Hydrogen-Air Mixtures Over An Isolated Vee-Gutter Flameholder Using a Well-Stirred Reactor Model." I have examined the final copy of this thesis for form and content and recommend that it be accepted in partial fulfillment of the requirements for the degree of Master of Science, with a major in Mechanical Engineering.

Dr. Roy J. Schulz, Major Professor

We have read this thesis and recommend its acceptance:

Accepted for the Council:

Associate Vice Chancellor
and Dean of The Graduate School

STATEMENT OF PERMISSION TO USE

In presenting this thesis in partial fulfillment of the requirements for a Master of Science degree at The University of Tennessee, Knoxville, I agree that the Library shall make it available to borrowers under the rules of the Library. Brief quotations from this thesis are allowable without special permission, provided that accurate acknowledgment of the source is made.

Permission for extensive quotation from or reproduction of this thesis may be granted by my major professor, or in his absence, by the Head of Interlibrary Services when, in the opinion of either, the proposed use of the material is for scholarly purposes. Any copying or use of the material in this thesis for financial gain shall not be allowed without my written permission.

Signature Julie N Darnell

Date 7/24/95

PREDICTION OF FLAME BLOWOFF LIMITS FOR HYDROGEN-AIR MIXTURES OVER AN ISOLATED VEE-GUTTER FLAMEHOLDER USING A WELL-STIRRED REACTOR MODEL

A Thesis

Presented for the

Master of Science

Degree

The University of Tennessee, Knoxville

Julie Ann Darnell

August 1995

DEDICATION

This thesis is dedicated to my parents,

Vernon and Marcella Darnell,

and to all of the friends I have made while on my

great adventure.

ACKNOWLEDGMENTS

I want to acknowledge the United States Air Force, Sverdrup Technology, Inc. and the University of Tennessee Space Institute for sponsoring this research. The research effort was conducted under a research assistantship at Arnold Engineering Development Center at Arnold Air Force Base, Tennessee. I want to thank my major professor, Dr. Roy Schulz, for his guidance and counsel and my other committee members, Dr. Roger Crawford and Dr. F. Shahrokhi, for their assistance. I also want to thank Scott Bartlett and Doug Garrard at Sverdrup for their assistance. I especially thank Dr. Edwin Gleason, Assistant Dean of Admissions at UTSI, for his concern for and dedication to students.

ABSTRACT

The purpose of this research was to begin initial development of an analytical tool to predict flame blowoff limits for hydrogen-air mixtures over vee-gutter flameholders. A specific geometric configuration of an isolated vee-gutter was selected to represent a flameholder test apparatus described in the literature. An analytical tool was developed by treating the recirculation zone behind the vee-gutter as a homogeneous chemical reactor, modeling the recirculation zone as a well-stirred reactor and using LSENS, a chemical kinetics code, to solve the governing equations of the reacting flow. The well-stirred reactor was assumed adiabatic and operated under steady-state conditions. The well-stirred reactor model was applied to premixed, turbulent hydrogen-air mixtures over the vee-gutter configuration. To calibrate the well-stirred reactor model, appropriate values of the recirculation zone volume from existing experimental data for hydrogen-air mixtures at given freestream static pressures were determined. The freestream, blowoff velocities were predicted for static pressures from 1.5 psia to 6 psia and static temperatures from 530 ^{o}R to 930 ^{o}R.

The blowoff limits predicted by LSENS were compared to existing experimental data on axisymmetrical disks corrected for two-dimensional flameholders at a given pressure. A parametric study of the model predictions was conducted to analyze the effects of pressure, temperature, fuel-air equivalence ratio and Reynolds number on flame stability. Conclusions were drawn regarding the accuracy and potential use of the model. The well-stirred reactor model developed in this study provides a useful preliminary survey of flame blowoff limits for premixed, turbulent hydrogen-air mixtures over the specific geometric configuration.

TABLE OF CONTENTS

CHAPTER		PAGE
1.	INTRODUCTION	1
2.	DEVELOPMENT OF THE ANALYTICAL TOOL TO PREDICT FLAME BLOWOFF LIMITS	6
	Flame Stabilization on a Bluff Body	6
	Well-Stirred Reactor Theory	9
	Description of the Chemical Kinetics Code	12
	Implementation of the Well-Stirred Reactor Model	12
3.	APPLICATION OF THE WELL-STIRRED REACTOR MODEL WITH SOLUTION BY LSENS	16
	Geometric Configuration of Vee-Gutter and Flow Field	16
	Aerothermodynamic Assumptions	18
	LSENS Input Parameters	19
4.	FLAME BLOWOFF LIMITS PREDICTED BY THE LSENS WELL-STIRRED REACTOR SOLUTION	27
5.	EVALUATION OF BLOWOFF PREDICTIONS FROM THE LSENS WELL-STIRRED REACTOR SOLUTION	30
	Conversion of LSENS Predictions to Blowoff Velocities	30
	Comparison of Predicted Blowoff Velocities from LSENS Solution to Calculations from DeZubay's β-Parameter	31
	Parametric Study of Predicted Flame Blowoff Limits	35
6.	CONCLUSIONS	38

LIST OF REFERENCES ____ 41

APPENDICES ____ 45

APPENDIX A. SAMPLE LSENS INPUT DATA FILE ____ 46

APPENDIX B. AERODYNAMIC WIDTH OF THE RECIRCULATION ZONE BEHIND THE SELECTED VEE-GUTTER ____ 49

APPENDIX C: EQUIVALENT DISK DIAMETER FOR SAME AERODYNAMIC BLOCKAGE AS ONE-FOOT SPAN OF VEE-GUTTER ____ 51

APPENDIX D. SAMPLE LSENS OUTPUT DATA FILE FOR APPARENT BLOWOUT CONDITION ____ 53

APPENDIX E. SAMPLE LSENS OUTPUT DATA FILE FOR NON-CONVERGENCE CONDITION ____ 58

APPENDIX F. DERIVATION OF THE EQUATION FOR BLOWOFF VELOCITY FOR THE REPRESENTATIVE GEOMETRIC CONFIGURATION ____ 63

VITA ____ 65

LIST OF TABLES

TABLE PAGE

1. Investigated Flow Conditions at the Minimum-Area of the Representative Geometric Configuration ____ 20

2. Range of Parameters in DeZubay's Flame Stability Experiments ____ 21

LIST OF FIGURES

FIGURE		PAGE
1.	Schematic of the Conceptual Design for Real-Time Afterburning of the Exhaust Gas in a Typical Altitude Test Facility	2
2.	Flame Stabilization on a Typical Vee-Gutter Flameholder	7
3.	Conceptual Schematic of a Well-Stirred Reactor	10
4.	Sketch of the Representative Geometric Configuration of the Vee-Gutter and Flow Field	17
5.	Sixth-Order Polynomial Fit of DeZubay's Experimental β-Parameter	22
6.	Proportionality Constant for the Reactor Volume versus Static Pressure at the Minimum-Area of the Geometric Configuration	25
7.	Blowoff Data for Hydrogen-Air Mixtures Predicted by LSENS Well-Stirred Reactor Solution with T_2=530 °R	28
8.	Blowoff Data for Hydrogen-Air Mixtures Predicted by LSENS Well-Stirred Reactor Solution with T_2=730 °R	28
9.	Blowoff Data for Hydrogen-Air Mixtures Predicted by LSENS Well-Stirred Reactor Solution with T_2=930 °R	29
10.	Comparison of Blowoff Velocity from LSENS Predictions at T_2=530 °R to Calculations from DeZubay's β-parameter	32
11.	Blowoff Reynolds Number from LSENS Predictions at T_2=530 °R	34
12.	Entrainment Proportion Required to Match LSENS Predictions at T_2=530 °R to Blowoff Velocities from DeZubay's Corrected Data	34
13.	Blowoff Velocities for Hydrogen-Air Mixtures over the Isolated Vee-Gutter with T_2=530 °R	35

14. Blowoff Velocities for Hydrogen-Air Mixtures over the Isolated Vee-Gutter with T_2=730 °R _____ 36

15. Blowoff Velocities for Hydrogen-Air Mixtures over the Isolated Vee-Gutter with T_2=930 °R _____ 37

NOMENCLATURE

A_f	projected frontal area of the vee-gutter flameholder (in^2)
A_1	cross-sectional area of the upstream flow field (in^2)
A_2	cross-sectional area of the minimum-area flow field (in^2)
a	speed of sound (ft/sec)
B_A	aerodynamic blockage of the vee-gutter
B_G	geometric blockage of the vee-gutter
C_D	drag coefficient of the vee-gutter
C_1	proportionality constant for the ratio of mass entrained into the recirculation zone of a vee-gutter flameholder
d	diameter of the axisymmetrical disk in DeZubay's experiments (in)
e_t	proportion of upstream mass flow through the projected area of the vee-gutter that is entrained into the recirculation zone
g_c	acceleration constant (32.174 lbm ft lbf^{-1} sec^{-2})
h_i	molar enthalpy of the ith species in the products of combustion (BTU/mol)
h_i^*	molar enthalpy of the ith species in the reactants of combustion (BTU/mol)
I	total number of species in the chemical reaction equation
J	total number of reactions
K	proportionality constant for the reactor volume
k_j	forward rate constant
k_{-j}	backward rate constant

L	length of the vee-gutter exposed to the hydrogen-air mixture
M	notation for the third body in the chemical reaction equation
m	mass flow rate of the unburned mixture into the well-stirred reactor (lbm/sec)
m_f	mass flow rate through the projected frontal area of flameholder (lbm/sec)
m_{ent}	mass entrained into the recirculation zone behind the vee-gutter (lbm/sec)
m_1	mass flow rate through the upstream flow field (lbm/sec)
m_2	mass flow rate through the minimum-area flow field (lbm/sec)
m_{max}	maximum mass flow rate for LSENS convergence (lbm/sec)
P_d	static pressure at the disk-duct minimum-area in DeZubay's experiments (psia)
P_1	static pressure of the upstream flow field (psia)
P_2	static pressure of the minimum-area flow field (psia)
ΔQ	heat added to or extracted from the well-stirred reactor (BTU)
R	specific gas constant of the fresh mixture (lbf ft (lbm $^oR)^{-1}$)
Re	Reynolds number
S	unit span of the vee-gutter flameholder (ft)
S_i	notation for the ith species in the chemical reaction equation
T_f	uniform static temperature of reacting mixture in the well-stirred reactor (^oR)
T_o	uniform static temperature of unburned mixture into the well-stirred reactor (^oR)
T_1	static temperature of the upstream flow field (^oR)
T_2	static temperature of the minimum-area flow field (^oR)
U_{bo}	blowoff velocity (ft/sec)

U_d velocity at the disk/duct minimum-area in DeZubay's experiments (ft/sec)

U_1 velocity of the upstream flow field (ft/sec)

U_2 velocity of the minimum-area flow field (ft/sec)

V_R volume of the well-stirred reactor (ft^3)

W width of the streamtube for the center flameholder in the vee-gutter array (in)

w width of the vee-gutter (in)

w_A aerodynamic width of the vee-gutter (in)

β DeZubay' flame stability parameter

γ ratio of specific heats

θ included angle of the vee-gutter (degrees)

μ coefficient of viscosity (lbf sec ft^{-2})

ν_{ij}' stoichiometric coefficient of the ith species in the reactants

ν_{ij}'' stoichiometric coefficient of the ith species in the products

ν_j stoichiometric coefficient of the third body in a reaction

ρ reacting gas density (lbm/ft^3)

σ_i concentration of the ith species in the products (mol/lbm)

σ_i^* concentration of the ith species in the reactants (mol/lbm)

σ_m sum of the product concentration (mol/lbm)

φ fuel-air equivalence ratio

CHAPTER 1

INTRODUCTION

As aeropropulsion technology expands to meet the challenges of the 21st Century, ground test capabilities of hydrogen-fueled aeropropulsion systems, such as ramjets and scramjets, are essential. Altitude-simulation testing of large-scale, hydrogen-fueled systems may be performed in existing ground test facilities; however, such testing may produce combustible mixtures of hydrogen and air in the facility exhaust ducting. Reduction of the level of hydrogen in facility exhaust systems to below flammability limits has been addressed by several researchers.[1, 2] One conceptual design involves controlled burning of the exhaust gas using an array of piloted, vee-gutter flameholders and is based on experience with gas turbine afterburners.[2] Figure 1 is a simple schematic of the conceptual design for real-time afterburning of the exhaust gas in a typical altitude test facility.[2] The burner in Figure 1 is the array of piloted, vee-gutter flameholders. Technical feasibility of the design is uncertain, principally due to the wide ranges of velocity, fuel-air ratios and static pressures that exist in such facility exhaust systems during operation.

Flammability limits for hydrogen-air mixtures are well documented at pressures near standard atmospheric;[3] however, hydrogen-air flammability limits are uncertain at the low pressures typically experienced in exhaust systems of altitude test facilities. Also, a significant amount of literature exists concerning flame stabilization on bluff bodies using conventional fuels of gas turbine engines. The literature concerning flame stabilization on bluff bodies referenced in this research is not exhaustive. Several researchers[4-8] have investigated flame stability of hydrocarbon fuels on axisymmetrical

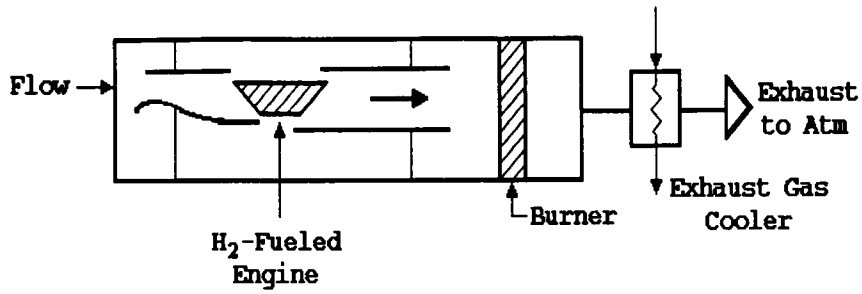

Figure 1: Schematic of the Conceptual Design for Real-Time Afterburning of the Exhaust Gas in a Typical Altitude Test Facility

Adapted from: G. Garrard and C. Bartlett, "Hydrogen Exhaust Gas Disposition by Afterburning," AIAA-91-5075, AIAA Third International Aerospace Planes Conference, Orlando, FL, December 3-5, 1991.

flameholders, (i.e., disks, cones, and cylinders). DeZubay[9, 10] conducted flame stabilization experiments with various fuels, including hydrogen, on axisymmetrical disks for a range of pressures. Lefebvre and others[11-14] have investigated flame stabilization on two-dimensional flameholders using hydrocarbon fuels. To the author's knowledge, however, the literature is deficient concerning flame stabilization of premixed, turbulent hydrogen-air mixtures over two-dimensional flameholders, such as vee-gutters. Due to these deficiencies, an analytical tool is desired for parametric investigation of flammability limits for premixed, turbulent hydrogen-air mixtures over vee-gutter flameholders. The analytical tool must be capable of parametric investigation for a range of flow conditions typically expected in exhaust systems of altitude test facilities.

The purpose of this research was to begin initial development of an analytical tool to predict flame blowoff limits for hydrogen-air mixtures over vee-gutter flameholders. Development of the analytical tool involved selecting a theoretical mechanism for flame stabilization, a mathematical model of the mechanism and a chemical kinetics code capable of solving the governing equations of the reacting flow. The selected theoretical

mechanism of flame stabilization treats the recirculation zone in the wake of the flameholder as a homogeneous chemical reactor. The well-stirred reactor theory provides a one-dimensional, mathematical model of homogeneous combustion. In the present study, the well-stirred reactor operates adiabatically under steady-state conditions. The well-stirred reactor model of the recirculation zone produced a governing set of non-linear, algebraic equations, which incorporate the conservation equations and the finite-rate chemical reaction kinetics. LSENS, the Lewis General Chemical Kinetics and Sensitivity Analysis Code,[15, 16] was used to solve governing equations of the model.

For a given flameholder configuration, implementation of the well-stirred reactor model reduces to two essential modeling requirements: (1) determining the mass entrainment rate of fresh mixture into the recirculation zone of the flameholder, and (2) determining the effective volume of the recirculation zone, the reactor volume. These two physical phenomena, along with the finite-rate chemical reaction kinetics of the mixture, determine the residence time of the reacting mixture in the recirculation zone. When residence time is less than the chemical induction time, steady-state combustion cannot be sustained and flame blowoff occurs. The chemical induction time is the time required for finite-rate, chemical reaction kinetics to reach a point where the system can proceed to completion or to a steady-state operation. Using correlation methods described in the literature, the mass entrainment rate was held constant at 10% of the upstream mass flow through the projected frontal area of the flameholder. Also from the literature, a relationship between the reactor volume and the square of the aerodynamic width of the recirculation zone was established.

In this modeling effort, a hypothesis was made that static pressure and Reynolds number effects on flame stabilization could be incorporated by empirical correlation with respect to mass entrainment rate and the reactor volume. That is, once a mass

entrainment rate and a reactor volume are determined at a design point, the blowoff limits at different pressures and Reynolds numbers could be determined from correlations derived from existing experimental or analytical data. The well-stirred reactor model was calibrated to the specific vee-gutter configuration by determining appropriate values of the reactor volume from existing experimental data for hydrogen-air mixtures at given freestream static pressures.

The well-stirred reactor model was applied to ignited, flowing hydrogen-air mixtures over an isolated vee-gutter flameholder. A specific geometric configuration of the vee-gutter and flow field was selected to represent the flameholder test apparatus described by Garrard and Bartlett.[2] Application of the model requires description of the geometric configuration, statement of the aerothermodynamic assumptions of the flow field and specification of the LSENS input parameters. The flame blowoff data for hydrogen-air mixtures predicted by the LSENS well-stirred reactor solution were plotted against the fuel-air equivalence ratio for freestream static pressures of 1.5 psia to 6 psia and freestream static temperatures of 530 °R to 930 °R.

Evaluation of the blowoff limits predicted by the well-stirred reactor model requires conversion of mass flow rate to velocity; therefore, an equation for blowoff velocity in terms of the blowoff mass flow rate predicted by LSENS, defined flow conditions, and the geometric configuration was derived. The blowoff velocities calculated from the LSENS predictions were compared to DeZubay's experimental disk data,[10] corrected for two-dimensional flameholders using a correction factor given by Zukoski.[17]

A parametric study of the predicted blowoff velocities was conducted to analyze the effects of mixture composition and freestream flow conditions on flame stability. The results of the parametric study are discussed. Conclusions regarding the accuracy and

potential use of the well-stirred reactor model are addressed. The well-stirred reactor model developed for solution by LSENS provides a preliminary model for predicting flame blowoff limits of premixed, turbulent hydrogen-air mixtures over isolated vee-gutter flameholders.

CHAPTER 2

DEVELOPMENT OF THE ANALYTICAL TOOL TO PREDICT FLAME BLOWOFF LIMITS

Development of the analytical tool to predict flame blowoff limits requires selection of a theoretical mechanism for flame stabilization on a bluff body, according to some model of reacting-flow physics. A mathematical model of the mechanism and a chemical kinetics code capable of solving the governing equations of the reacting flow were then selected accordingly. Theoretical considerations involved in the development of the analytical tool were adapted from previous works and applied to two-dimensional flameholders, specifically vee-gutters.

FLAME STABILIZATION ON A BLUFF BODY

With the advent of augmented gas turbines, flame stabilization on bluff bodies has been studied extensively. Figure 2 is a sketch of a physical model for flame stabilization on a vee-gutter flameholder adapted from Ozawa.[18] The flameholder produces in its wake a region of recirculating flow where the flow velocity is less than the burning velocity of the mixture. The main flame is initiated in the free shear layer and continues downstream. Once the mixture is ignited, the recirculation zone acts as a pilot, igniting the fresh mixture in the shear layer and anchoring the flame to the flameholder.[11] The effects of flame velocity relative to the flame stability of hydrogen-air mixtures will be discussed later. Regardless of the reacting mixture, however, vee-gutters in test facility exhaust systems will almost certainly be immersed in turbulent flows and have

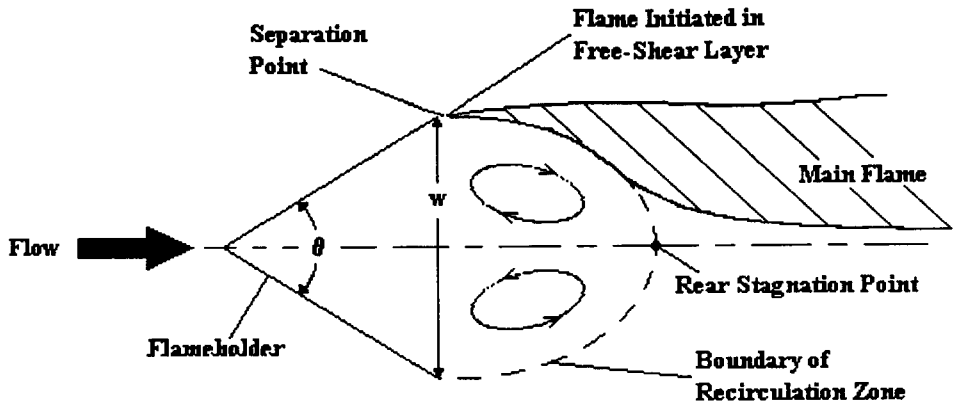

Figure 2: Flame Stabilization on a Typical Vee-Gutter Flameholder

Adapted from: *R. I. Ozawa, "Survey of Basic Data on Flame Stabilization and Propagation for High Speed Combustion Systems," Technical Report AFAPL-TR-70-81, The Marquardt Company, Wright-Patterson Air Force Base, OH, January 1971.*

turbulent wake regions; therefore, for this study, turbulent flame velocities are relevant to the determination of blowoff velocity. For flame propagation at sufficiently high pressures, turbulent flame velocities depend primarily on the turbulence level of the freestream and of the wake and to a lesser degree on the molecular transport properties that strongly influence laminar flame velocities.

Expression of the flame stabilizing performance of a bluff body usually takes the form of: (1) the range of fuel-oxidant equivalence ratios over which stable combustion in the wake is achieved, and (2) the maximum flow velocity that the bluff-body system can tolerate before flame extinction.[11] As the flow velocity increases, the residence time for the reacting mixture in the recirculation zone decreases for steady operation because mass entrained in the recirculation zone of the flameholder is proportional to freestream flow velocity. The blowoff velocity is reached when the residence time of the reacting mixture is less than the

chemical induction time and/or when heat losses are great enough to thermally quench the flame. For either situation, individually or in combination, the chemical reaction kinetics cannot sustain stable combustion and flame extinction occurs. In the present study, heat losses from the recirculation zone are neglected

Previous studies of flame stabilization on bluff bodies are almost exclusively experimental and are concerned with the mean flow characteristics of the near wake, the region immediately downstream from the bluff body. These near-wake aerodynamic characteristics include flow separation and stagnation, velocity and pressure distribution, eddy formation, and transport and exchange processes.[8] Aerodynamic characteristics largely determine the mechanism of flame stabilization on the bluff body and depend on the flow conditions and turbulence levels of the freestream, as well as body geometry. Presently, local characteristics of turbulent flows rely on experimental investigation and cannot be generally predicted.[8] Historically, however, the theoretical study of the mechanism of flame stabilization on a bluff body takes two basic approaches.[11]

The first theoretical description of the mechanism of flame stabilization was reported by Longwell and associates.[19] Following this approach, the recirculation zone of the flameholder is the focus of study. Analysis of the flame stabilizing mechanism involves viewing the recirculation zone as a homogeneous chemical reactor. Flame blowoff occurs when the residence time of combustion gases in the recirculation zone is less than the time necessary to raise the temperature of the gases in the recirculation zone to the ignition temperature.

A second, more involved description was reported by Zukoski and Marble.[20] Following this approach, the free shear layer surrounding the recirculation zone is the focus of study. Fresh mixture from the freestream is

entrained into the shear layer and ignited by turbulent mixing with previously ignited, hot combustion products from the recirculation zone. The burning mixture in the shear layer propagates downstream igniting the neighboring fresh mixture in the freestream. At the end of the wake, some of the burning mixture is entrained into the recirculation zone while the remainder continues downstream. The recirculating flow conveys the burning mixture upstream through the recirculation zone where it ignites the fresh mixture in the shear layer. This cyclic process is the mechanism of flame stabilization. Flame blowoff occurs when the residence time of fresh mixture in the shear layer is less than the delay time for ignition of the fresh mixture by hot combustion products from the recirculation zone.

Coupled together, these two theoretical approaches explain the physics of flame stabilization on a bluff body; however, on the basis of model simplicity, the author selected the theoretical mechanism proposed by Longwell and associates to physically model flame stabilization on a vee-gutter. Also, on the basis of historical precedence in the literature,[12, 21] the author selected the well-stirred reactor theory to mathematically model the recirculation zone of the flameholder as a homogeneous chemical reactor.

WELL-STIRRED REACTOR THEORY

The well-stirred reactor, developed by Longwell and Weiss,[22] is a one-dimensional, mathematical model for steady, homogeneous combustion. In the well-stirred reactor, the rate of mixing is assumed to be infinite; therefore, the combustion gases in the reactor are homogeneous with uniform temperature and pressure. Figure 3 shows a conceptual schematic of a well-stirred reactor.

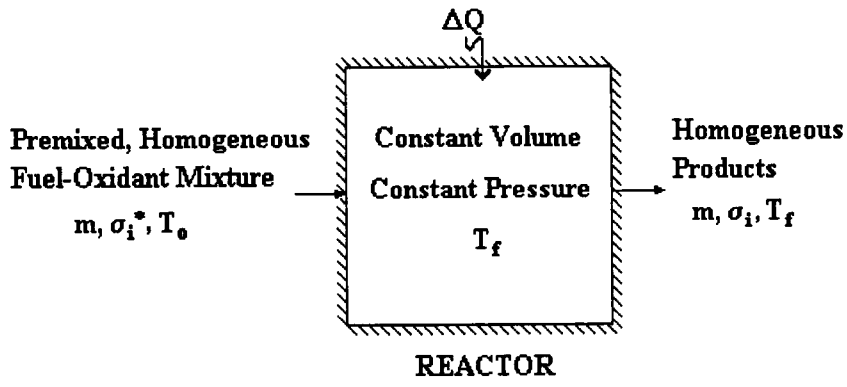

Figure 3: Conceptual Schematic of a Well-Stirred Reactor

The premixed, homogeneous mixture containing I species denoted by S_i (i=1,2,...I) enters the reactor volume, V_R, at a specified mass flow rate, m, and uniform inlet temperature, T_o. The concentration of each reactant species entering the reactor is σ_i^*. The constant volume reactor contains combustion gases at constant pressure and uniform temperature, T_f. Heat, ΔQ, may be added to or extracted from the reactor volume, or, as in the present study, the reactor may be adiabatic. For steady operation, the combustion products exit the reactor at a mass flow rate, m, and uniform temperature, T_f. The concentration of each product species leaving the reactor is σ_i.[23]

Defining M as a third body and S_i as the ith species (i=1,2,...I) in the premixed, homogeneous mixture, the general reaction mechanism,[23] containing J reactions, is given by:

$$\Sigma_i(\nu_{ij}' S_i + \nu_j M) <=> \Sigma_i(\nu_{ij}'' S_i + \nu_j M) \quad \text{where } j=1,2,...J \qquad (2.1)$$

For a given set of chemical reaction kinetics and steady operation, the continuity equation[23] for each reacting species is given by:

$$m(\sigma_i-\sigma_i^*)/V_R = -\rho^2 \Sigma_j\{(\nu_{ij}''-\nu_{ij}')[k_j(\rho\sigma_m)^{\nu_j} \Pi_i(\rho\sigma_i)^{\nu_{ij}'}-k_{-j}(\rho\sigma_m)^{\nu_j} \Pi_i(\rho\sigma_i)^{\nu_{ij}''}]\} \quad (2.2)$$

For a given set of chemical reaction kinetics and steady operation, the conservation of energy equation[23] for each reacting species in a well-stirred reactor is given by:

$$m \Sigma_i(\sigma_i h_i - \sigma_i^* h_i^*) = -\Delta Q \quad (2.3)$$

Assuming ideal gas behavior, $h_i^* = h_i^*(T_o)$ and $h_i = h_i(T_f)$.

Combining Equations 2.2 and 2.3 with the chemical reaction kinetics of a given combustible mixture produces a set of non-linear, algebraic equations that can be solved numerically.

An emphasis must be made that the well-stirred reactor theory is one-dimensional in time; therefore, the theory represents "no-flow" combustion and is not concerned with the conservation of momentum. The reactants enter the reactor volume; uniform, homogeneous combustion occurs, and the products exit the reactor volume, all under constant pressure conditions. As mentioned previously, in the case of two-dimensional flow over vee-gutters, the near-wake aerodynamics are changing with changes in flow velocity and freestream turbulence levels. The near-wake aerodynamics are governed by the conservation of mass, momentum and energy. Inclusion of the aerodynamic effects involved in the conservation of momentum is beyond the capability of the simple well-stirred reactor theory; therefore, detailed predictions of the near-wake aerodynamics are unnecessary.

For blowoff prediction, the principal physical parameters accounted for by the well-stirred reactor model are:

- The chemical composition of the mixture (i.e., the species present).
- The stoichiometry of the unburned mixture (i.e., the fuel-oxidant equivalence ratio).
- The inlet static pressure and temperature to the reactor.
- The mass flow rate into the reactor volume.
- The heat transfer to or from the reactor volume.

A general chemical kinetics code was selected for numerical correlation of the effects of the preceding parameters on flame blowoff limits.

DESCRIPTION OF THE CHEMICAL KINETICS CODE

The author selected a general chemical kinetics program entitled the Lewis General Chemical Kinetics and Sensitivity Analysis Code (LSENS) to solve the set of governing equations of the well-stirred reactor model. LSENS was developed at the NASA Lewis Research Center. References 15 and 16 contain detailed description of the employment of LSENS. LSENS utilizes a Newton-Raphson iterative procedure in the well-stirred reactor solution. The application of the LSENS well-stirred reactor solution in determining flame stability is discussed in more detail in the following chapter.

IMPLEMENTATION OF THE WELL-STIRRED REACTOR MODEL

With the selection of LSENS, implementation of the well-stirred reactor model reduces to two essential modeling requirements: (1) determining the mass entrainment rate of fresh mixture into the recirculation zone, m_{ent}, and (2) determining the effective volume of the recirculation zone, the reactor volume,

V_R. These two physical phenomena, along with the finite-rate chemical reaction kinetics of the mixture, determine the residence time of the reacting mixture in the reactor volume. In this modeling effort, a hypothesis was made that static pressure and Reynolds number effects on flame stabilization could be incorporated by empirical correlation with respect to m_{ent} and V_R. That is, once m_{ent} and V_R are determined at a design point, the blowoff limits at different pressures and Reynolds numbers can be determined from correlations derived from existing experimental or analytical data.

Although several researchers have investigated near-wake characteristics of axisymmetrical flameholders in ducted flow,[4-10, 21] to the author's knowledge, there is insufficient experimental or analytical data to precisely quantify the effects of pressure and Reynolds number on both m_{ent} and V_R for turbulent flows over two-dimensional flameholders. Using existing data, however, pressure effects are more easily correlated than Reynolds number effects; therefore, the effects of Reynolds number are initially neglected in the determination of m_{ent} and V_R. Pressure effects on blowoff, except those that arise from the chemical reaction kinetics and for which LSENS accounts, can be correlated by determining either $m_{ent} = m_{ent}(P_2)$ or $V_R = V_R(P_2)$. That is, either m_{ent} or V_R can be corrected for local static pressure effects (by comparison with existing data) but not both. The author, therefore, selected a constant correlation between m_{ent} and static pressure and then determined $V_R = V_R(P_2)$ from existing experimental data.

The appropriate values of m_{ent} and V_R for ducted flow over vee-gutters were determined using correlation methods described in the literature. Several researchers have addressed entrainment rates of the fresh mixture into the near

wakes of bluff bodies. The following discussion concerning fresh-mixture entrainment is not exhaustive; however, since entrainment rate correlations are dependent on experimental test configurations, the following represents the literature referenced in this study.

Roberds, et. al.,[21] experimentally investigated the residence times, air entrainment rates, and base pressures in the near wake of an axisymmetrical cylinder in subsonic flow. The investigation was conducted under cold flow conditions. The researchers assumed that the mass entrained into the near wake was a proportion of the upstream mass flow through the projected frontal area of the cylinder. The residence time over a range of flow conditions was measured experimentally. The reciprocal of the residence time was plotted against the freestream air velocity corrected by the ratio of total and static temperatures. The proportion entrained into the near wake was calculated from the slope of the linear best-fit through the data. For the particular test configuration in this experimental study, the proportion of mass entrained into the near wake of the cylinder was approximately 8% of the upstream flow through the projected frontal area of the cylinder.

Using a hydrocarbon fuel, Baxter and Lefebvre[12] include an empirical correlation for the proportion of mass entrained into the recirculation zone of a vee-gutter as a function of θ, B_G, and upstream velocity and temperature. The correlation, converted to English units and the nomenclature provided in this work, is given by:

$$m_{ent}/m_1 = 2.111\ C_1[0.155+0.08(\theta/30 -1)][B_G/(1-B_G)(U_1/T_1^{0.75})] \qquad (2.4)$$

Equation 2.4 does not directly include pressure effects. For this study, the proportionality constant, C_1, was assumed equal to unity to allow one-to-one corrections later in the analysis. For the configuration and range of flow conditions described in the following chapter, Equation 2.4 predicts entrainment of approximately eight to twelve percent of the upstream flow. Since Equation 2.4 deals specifically with vee-gutters, the author selected a mean entrainment of 10%. For all subsequent calculations, the proportion of mass, e_t, entrained into the recirculation zone was held constant at 10% of the upstream flow through the projected, frontal area of the vee-gutter over the entire range of static pressures.

For a vee-gutter flameholder, Baxter and Lefebvre[12] state that the volume of the recirculation zone per unit span of the flameholder is proportional to the square of the aerodynamic width of the recirculation zone. Defining a proportionality constant, K, the relation for V_R becomes:

$$V_R/S = K(w_A^2) \tag{2.5}$$

With the assumption that V_R depends on static pressure, an empirical correlation of K with respect to static pressure can be determined from existing experimental data for hydrogen-air mixtures over bluff bodies. Also, the empirical correlation of K can be used to calibrate the well-stirred reactor model to the specific geometric configuration described in the following chapter.

CHAPTER 3

APPLICATION OF THE WELL-STIRRED REACTOR MODEL WITH SOLUTION BY LSENS

The well-stirred reactor model, as outlined in the previous chapter, was applied to ignited, flowing hydrogen-air mixtures over an isolated vee-gutter flameholder. A specific geometric configuration of the vee-gutter and flow field was selected to represent the flameholder test apparatus described by Garrard and Bartlett.[2] Application of the model requires description of the geometric configuration, statement of the aerothermodynamic assumptions of the flow field and specification of the LSENS input parameters.

GEOMETRIC CONFIGURATION OF VEE-GUTTER AND FLOW FIELD

For this study, the author adapted a vee-gutter configuration from the design of a hydrogen exhaust gas disposition test reported by Garrard and Bartlett.[2] As reported, a small, research test facility was designed to investigate the flammability limits of premixed, turbulent, hydrogen-air mixtures over an array of piloted, vee-gutter flameholders. For convenience in later calculations, the following geometric measurements were assumed exact. To represent vee-gutter array configurations typical of gas-turbine augmentors, a configuration was selected that produced a 30% geometric blockage, B_G, of the flow. At the base, the width of the vee-gutter was 1.5 inches with a 30° included angle. The length, or span, of the flameholder exposed to the hydrogen-air mixture was 4 inches. To produce B_G=0.3, the width of the streamtube for the vee-gutter was 5 inches. The

boundaries of the stream tube are assumed fixed and, for the purpose of modeling, are representative of ducted flow. Figure 4 is a sketch of the representative geometric configuration of the vee-gutter and flow field

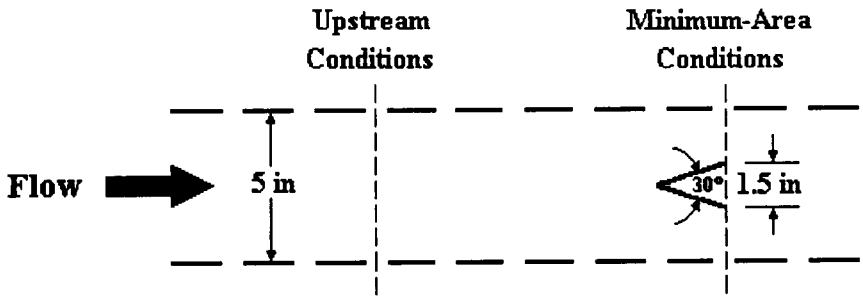

Figure 4: Sketch of the Representative Geometric Configuration of the Vee-Gutter and Flow Field

A strong emphasis must be made that, although real augmentors generally consist of an array of flameholders, the present study is concerned only with a single, isolated vee-gutter. The well-stirred reactor model, herein developed, strictly applies to only an isolated vee-gutter; however, empirical corrections to the near-wake aerodynamics, namely the mass entrainment into the wake and the effective volume of the wake, can account for array and blockage effects. Any influences on near-wake aerodynamics due to the proximity of other vee-gutters in a real array are beyond the scope of this study. When blockage effects of flameholders in ducted, subsonic flows cause increases in the flow velocity, a velocity correction based on Mach number and area ratio is possible since the flow outside the vee-gutter wake is isentropic. Note that the critical, upstream Mach number for ducted flow with 30% blockage is 0.46.[24]

AEROTHERMODYNAMIC ASSUMPTIONS

The recirculation zone of the previously defined vee-gutter was mathematically modeled as a well-stirred reactor. The model assumes the following conditions:

- Hydrogen-air flow from upstream to the minimum-area is steady, compressible, isentropic and inviscid.
- Total pressure and total temperature remain unchanged between upstream and minimum-area conditions.
- The hydrogen-air mixture is an ideal gas.
- Air has a standard composition with inert, trace species of Ar and CO_2.
- The pressure at the minimum-area and the pressure at the base of the flameholder are equal.
- The recirculation zone is an adiabatic ($\Delta Q=0$), constant pressure, constant volume reactor at a given operating point.

The previously stated assumptions simplify the governing equations of the well-stirred reactor model. Steady, compressible, isentropic, inviscid flow allows application of the relative thermodynamic relations between the upstream and minimum-area conditions. Constant total conditions provide a known condition for the thermodynamic relations. The ideal gas assumption allows application of the ideal gas flow equations, such as the equation of state ($P=\rho RT$) and the speed of sound ($a=\{\gamma g_c RT\}^{0.5}$). Standard composition of air with inert, trace species of Ar and CO_2 simplifies the chemical reaction kinetics of hydrogen-air combustion. From correlations given by Roberds, et. al.,[21] the percent difference between the pressure at the minimum-area and the base pressure of the flameholder is less than

7.5%; therefore, equality of the two pressures is a reasonable assumption. The assumption of an adiabatic, constant pressure, constant volume reactor simplifies the conservation equations.

LSENS INPUT PARAMETERS

Implementation of LSENS requires the following inputs:

- The fuel-air equivalence ratio of the unburned mixture.
- The inlet static pressure and temperature to the reactor.
- The chemical reaction kinetics of the combustible mixture.
- The initial mass flow rate into the reactor volume.
- The final mass flow rate into the reactor volume.
- An incremental mass flow rate for LSENS iteration on mass flow rate into the reactor volume.
- The reactor volume.

Investigated Flow Conditions

The author investigated the flame blowoff limits for flow conditions where flammability of hydrogen-air mixtures is uncertain, that is at low pressures and temperatures. For input to the LSENS well-stirred reactor model, the equivalence ratio and inlet static conditions are defined as the freestream flow conditions at the minimum-area of the selected geometric configuration. The flow conditions included in this study are listed in Table 1.

Table 1: Investigated Flow Conditions at the Minimum-Area of the Representative Geometric Configuration

PARAMETER	RANGE
Static Pressure	1.5 - 6 psia
Static Temperature	530 - 930 ^{o}R
Equivalence Ratio	0.2 - 2

Chemical Kinetics of Hydrogen-Air Mixtures

A standard set of chemical kinetic relations for hydrogen-air combustion, with Ar and CO_2 inert, was given in a LSENS program test case.[16] This set of chemical kinetics was used in all subsequent LSENS solutions. Appendix A contains a sample of LSENS input data, which includes the set of the chemical kinetic relations for hydrogen-air combustion.

Determination of Reactor Volume

The accurate performance of LSENS requires a reasonable value for reactor volume, which is the effective volume of the recirculation zone behind the vee-gutter. As expressed in Equation 2.5, the volume of the recirculation zone per unit span of the flameholder is proportional to the square of the aerodynamic width of the recirculation zone. Appendix B contains the calculation of w_A using correlations given by Baxter and Lefebvre.[12] The resulting value of w_A was 1.9 inches. Baxter and Lefebvre do not define the proportionality constant in Equation 2.5; therefore, at a design point, the value of the constant was estimated using existing experimental data for flame stability of hydrogen-air mixtures.

DeZubay [10] conducted flame stabilization experiments with several fuels, including hydrogen, on axisymmetrical disks in ducted flow. The disks were placed perpendicular to the flow direction and concentric with a circular duct. The fuel-air mixtures were premixed and homogeneous with a flat velocity profile approaching the disk. DeZubay used 99.7% pure hydrogen. For hydrogen-air mixtures, DeZubay conducted blowoff experiments for the range of parameters listed in Table 2.

Table 2: Range of Parameters in DeZubay's Flame Stability Experiments

PARAMETER	RANGE
Diameter of Disk	0.125, 0.250, 0.500 in.
Maximum Velocity	874 ft/sec
Static Pressure	2 - 6 psia
Static Temperature	550 +/- 30 °R

Source: E. A. DeZubay, "A Study of Flame Stability Based on Reaction Rate Theory," ASME Paper 54-SA-27, Presented at the Semi-Annual Meeting, Pittsburgh, PA, June 20-24, 1954.

For all experiments using hydrogen, the inner diameter of the circular duct was 1.32 inches, which produced geometric blockages of approximately 1 to 14 percent, respectively for the disk diameters shown above.

For hydrogen-air mixtures, DeZubay developed the following correlation for flame stability:

$$\beta = U_d / (P_d^{0.61}\, d^{0.74}) \qquad (3.1)$$

where U_d is in ft/sec, P_d is in psia and d is in inches.

In DeZubay's experiments, β was determined as a function of mass fuel-air ratio. Because freestream, static temperature was essentially constant in DeZubay's experiments, Equation 3.1 does not include effects of freestream, static temperature on flame stability.

A sixth-order polynomial fit of DeZubay's data, as a function of equivalence ratio, is given by:

$$\beta = -31.35 - 390.7\,\varphi + 3524\,\varphi^2 - 3669\,\varphi^3 + 1574\,\varphi^4 - 306.2\,\varphi^5 + 21.62\,\varphi^6 \qquad (3.2)$$

Figure 5 is a plot of the sixth-order polynomial fit of DeZubay's experimental data.

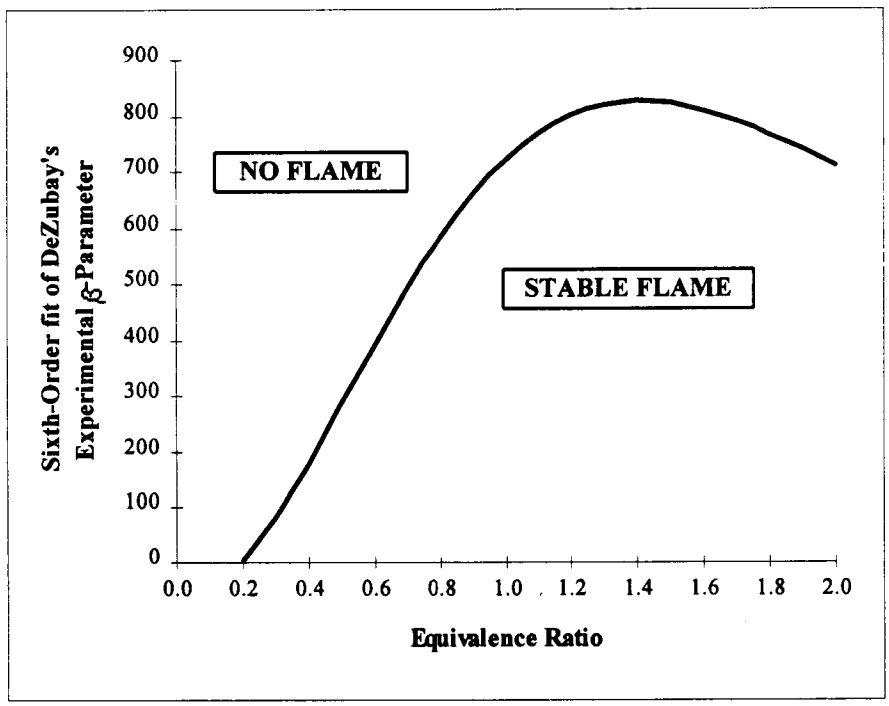

Figure 5: Sixth-Order Polynomial Fit of DeZubay's Experimental β-Parameter

To determine the flame stability at a specified value of φ and given values of U_d, P_d, and d, β is calculated from Equation 3.1. If the calculated value of β lies below the curve in Figure 5, the flame is stable. If the calculated value of β lies on or above the curve in Figure 5, the flame is unstable, and flame extinction occurs.

As discussed earlier, vee-gutters in test facility exhaust systems will be immersed in turbulent flows and have turbulent wake regions. Hydrogen has turbulent-flow, flame velocities up to 30 ft/sec,[25] which allows high flow velocities before flame extinction occurs. DeZubay's experimental blowoff data indicate that turbulent, hydrogen-air mixtures do have very high blowoff velocities.

Unfortunately for two-dimensional analysis, DeZubay obtained this experimental hydrogen-air blowoff data using axisymmetrical disks. For hydrocarbon fuels, however, Zukoski[17] analyzed the effects of blockage and flameholder geometry on flame stabilization for various bluff body configurations. Zukoski concluded that the maximum approach, or blowoff, velocity for an axisymmetrical flameholder is 50% greater than that of a two-dimensional flameholder, for comparable aerodynamic blockages. Zukoski's analyses were supported by experimental data reported by Wright.[26]

Given the work of Zukoski, DeZubay's experimental data may be used as a calibration benchmark for vee-gutter flame stabilization of hydrogen-air mixtures. First, however, the equivalent value of disk diameter, d, to produce the same aerodynamic blockage as the selected vee-gutter must be determined. From DeZubay's experiments using a

commercial grade of propane,[9] the aerodynamic diameter of a flat disk is approximately 1.8 times the diameter of the disk; therefore, a value of d=1.5 inches (see Appendix C) will produce the same aerodynamic blockage of the flow field as one-foot span of the selected vee-gutter.

The well-stirred reactor model can now be calibrated to the specific vee-gutter configuration by determining appropriate values of V_R from DeZubay's experimental data for hydrogen-air mixtures at given freestream static pressures. Using Equation 3.2, the value of β was calculated over the range of φ given in Table 1. The value for blowoff velocity at φ=1.2, P_d=P_2=3 psia and d=1.5 inches was then calculated using Equation 3.1 and corrected for vee-gutters. Given the geometric configuration and a constant e_t of 10%, the corrected blowoff velocity was converted to mass flow rate using the derived equation for blowoff velocity, which is detailed in the following chapter. Using LSENS and iterating on V_R, the author determined that V_R=0.00303 ft^3 resulted in blowoff at the calculated mass flow rate for 3 psia. As stated previously, V_R is a function of static pressure; therefore, at φ=1.2 and d=1.5 inches, the author similarly determined V_R for 1.5 psia, 4.5 psia and 6 psia. Equation 2.5 was then used to calculate the corresponding values of K. Figure 6 is a plot of K with respect to the freestream, static pressure at the minimum-area of the geometric configuration.

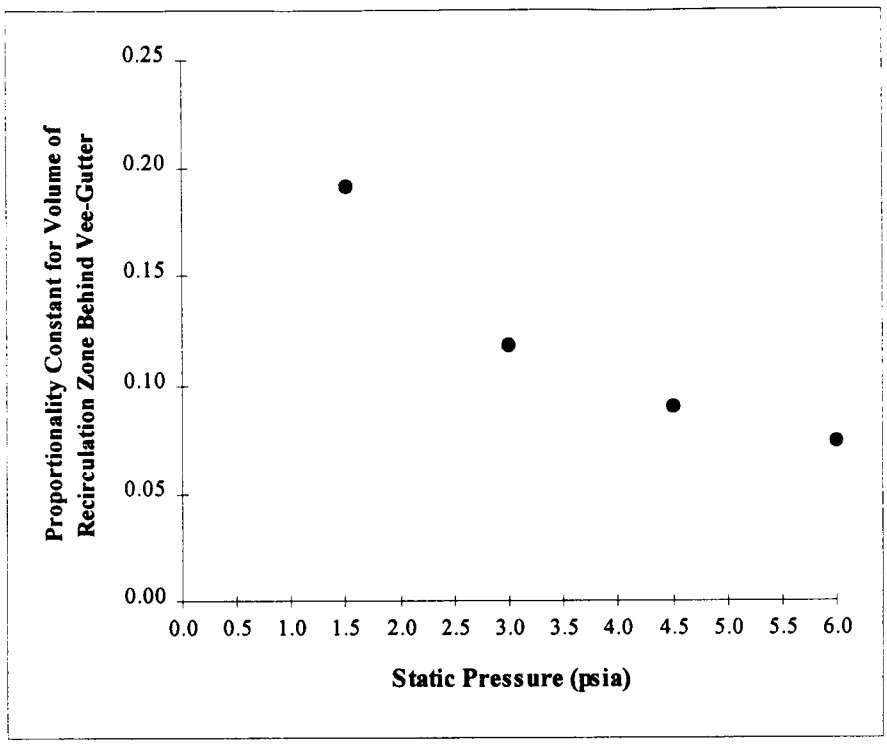

Figure 6: Proportionality Constant for the Reactor Volume versus Static Pressure at the Minimum-Area of the Geometric Configuration

A curve fit of the data in Figure 6 resulted in the following equation for K as a function of static pressure at the flameholder minimum-area:

$$K = \log^{-1}[-0.597 - 0.689 \log(P_2)] \qquad (3.3)$$

Equation 3.3 shows a logarithmic relationship between the proportionality constant of Equation 2.5 and the static pressure; therefore, for a given geometric configuration, V_R varies logarithmically with static pressure, based on DeZubay's experimental data for hydrogen air mixtures. From DeZubay's experimental data at a single operating point, the calculated values of V_R at the respective static pressures were used as the reactor

volume in the LSENS program for the full range of φ. Corrections to V_R with respect to Reynolds number effects were not addressed.

Iteration on Mass Flow Rate

LSENS solves the governing equations of the well-stirred reactor model for the initial mass flow rate. LSENS then increases the mass flow rate by an incremental value and performs another well-stirred reactor solution. LSENS continues to iterate on the mass flow rate until a fatal error occurs or the final mass flow rate is exceeded. At each mass flow rate, the program outputs either residence time and outlet flow conditions for a predicted stable flame or one of two fatal error messages that indicate a no-flame condition. One error message is 'Apparent Blowout'. This message occurs when the converged temperature is not much greater than the inlet temperature and indicates that a drastic drop in outlet temperature from the previous solution has occurred. Appendix D contains a sample LSENS output data file for the 'Apparent Blowout' condition. The other error message is 'Non-Convergence'. This message occurs when the solution does not converge after 75 iterations. Private communication with the program author[27] confirmed that the 'Non-Convergence' message also indicates a no-flame condition. Appendix E contains a sample LSENS output data file for the 'Non-Convergence' condition.

CHAPTER 4

FLAME BLOWOFF LIMITS PREDICTED BY THE LSENS WELL-STIRRED REACTOR SOLUTION

The author generated flame blowoff data for hydrogen-air mixtures by application of the well-stirred reactor model with solution by LSENS. The data were generated over the entire range of φ for several pressures and temperatures, as defined in Table 1. The data were generated based on a constant entrainment proportion of 10% and a reactor volume calibrated from DeZubay's experimental data. Note that the reactor volume was determined per one-foot span of vee-gutter. The maximum mass flow rate, m_{max}, resulting in convergence of the LSENS well-stirred reactor solution, was interpreted to be the limiting mass flow rate entrained into the recirculation zone that produced a stable flame per one-foot span of the vee-gutter.

Figure 7 is the plot of m_{max} for hydrogen-air mixtures predicted by the LSENS well-stirred reactor solution with T_2=530 ^oR; Figure 8 is the plot of m_{max} predicted by the LSENS well-stirred reactor solution with T_2=730 ^oR, and Figure 9 is the plot of m_{max} predicted by the LSENS well-stirred reactor solution with T_2=930 ^oR. For all flow conditions, the LSENS well-stirred reactor solution produced maximum m_{max} at stoichiometric conditions(i.e., φ=1.0).

The values plotted in Figures 7 show a discontinuity in the data at $0.3<\varphi<0.4$ for all pressures. In Figures 8 and 9, the discontinuity does not occur even for low pressure.. The discontinuity in the data at low temperature is a result of chemical induction time and is discussed more fully in the following chapter.

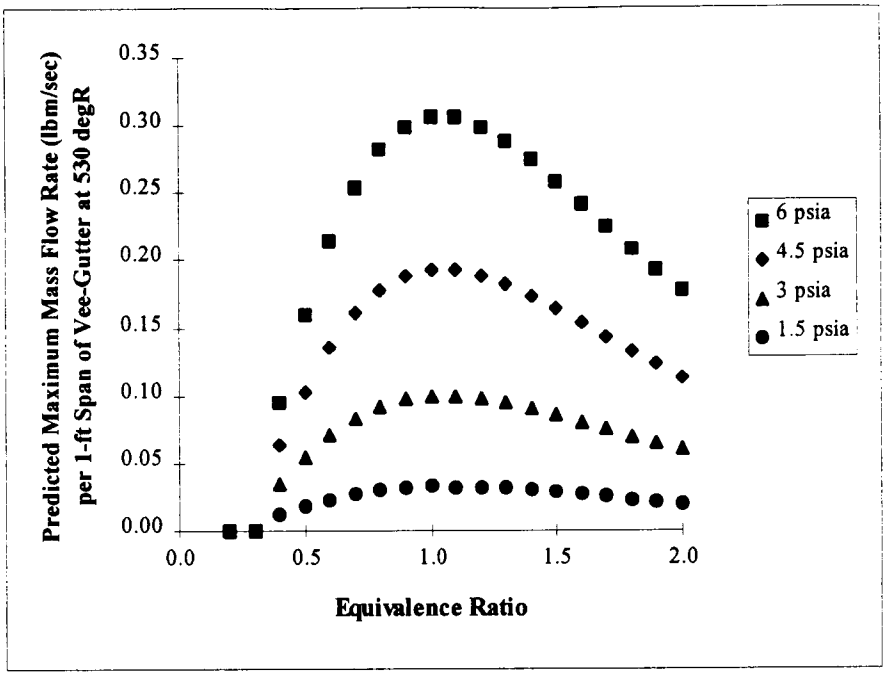

Figure 7: Blowoff Data for Hydrogen-Air Mixtures Predicted by LSENS Well-Stirred Reactor Solution with T_2=530 °R

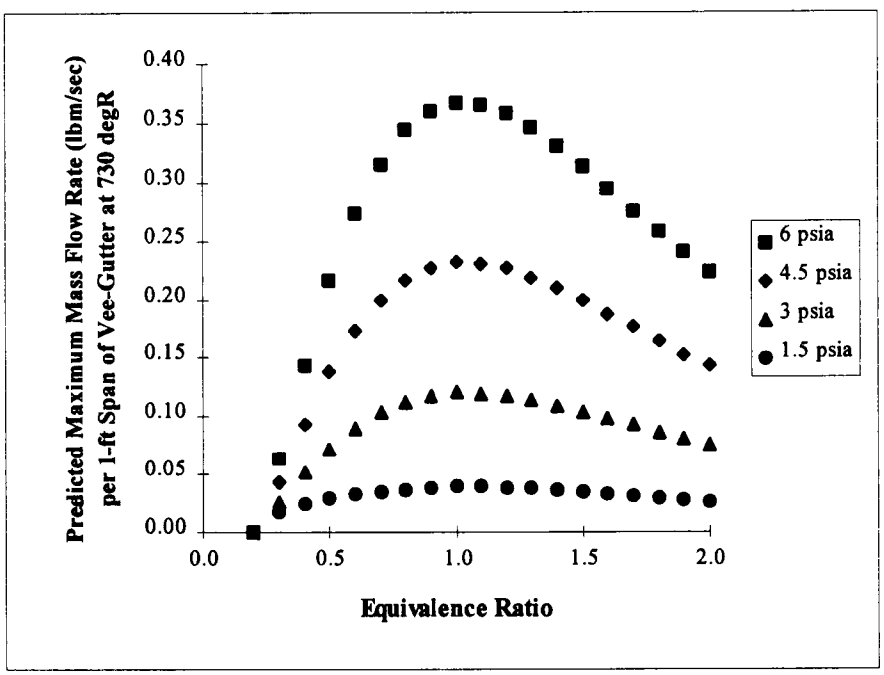

Figure 8: Blowoff Data for Hydrogen-Air Mixtures Predicted by LSENS Well-Stirred Reactor Solution with T_2=730 °R

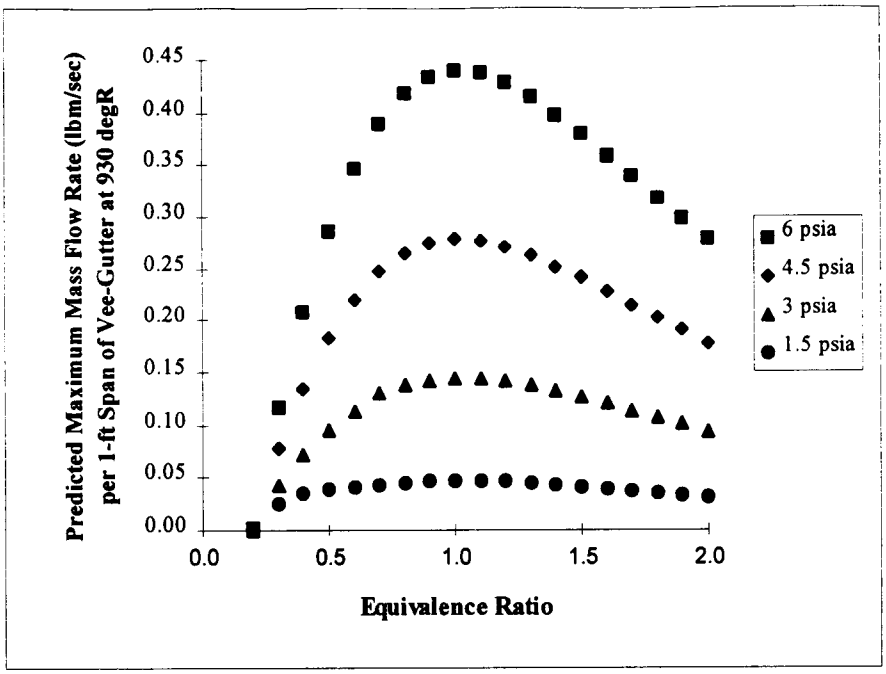

Figure 9: Blowoff Data for Hydrogen-Air Mixtures Predicted by LSENS Well-Stirred Reactor Solution with T_2=930 °R

CHAPTER 5

EVALUATION OF BLOWOFF PREDICTIONS FROM THE LSENS WELL-STIRRED REACTOR SOLUTION

The flame blowout limits predicted by the LSENS well-stirred reactor solution were evaluated using existing data. For quantitative evaluation, the values of m_{max} reported in the previous chapter were converted to blowoff velocities relative to the selected vee-gutter configuration. The author compared the U_{bo} calculated from the LSENS predictions to DeZubay's experimental disk data corrected for two-dimensional flameholders. The author conducted a parametric study of the values U_{bo} calculated from the LSENS predictions to analyze the effects of pressure, temperature and fuel-air equivalence ratio on flame stability.

CONVERSION OF LSENS PREDICTIONS TO BLOWOFF VELOCITIES

A correlation between U_{bo} and the m_{max} predicted by LSENS was developed. As detailed in the previous chapter, m_{max} was determined from LSENS for various pressures and temperatures at each respective reactor volume, based on S=1 ft. From the geometric configuration given in Chapter 3, the length of the vee-gutter exposed to the hydrogen-air mixture is 4 inches; therefore, the actual mass entrained behind the given vee-gutter is one-third the m_{max} predicted by LSENS. This method for developing the velocity correlation allows a relationship between vee-gutter geometry and ducted flow conditions (i.e., blockage, minimum-area flow conditions, etc.) that directly correlates the velocity at the minimum-area to the mass entrainment rate at blowoff. As detailed in

Chapter 2, Roberds, et al.,[21] state that the mass entrained behind a flameholder is some proportion of the upstream mass flow through the projected frontal area of the flameholder, and from Baxter and Lefebvre,[12] e_t was set at 10%. For the selected vee-gutter configuration, Appendix F contains the derivation of the equation for blowoff velocity in terms of m_{max}, e_t, B_G and the minimum-area flow conditions. The equation for blowoff velocity is given by:

$$U_{bo} = (m_{max} R T_2) / (3 e_t P_2 A_2 B_G) \qquad (5.1)$$

For the selected geometric configuration, A_2=14 in^2 and B_G=0.3. The specific gas constant, R, is a function of φ.

COMPARISON OF PREDICTED BLOWOFF VELOCITIES FROM LSENS SOLUTION TO CALCULATIONS FROM DEZUBAY'S β-PARAMETER

The blowoff velocities calculated from Equation 5.1 were compared to DeZubay's experimental disk data corrected for two-dimensional flameholders. Given the selected vee-gutter configuration, the calculation of blowoff velocity from DeZubay's data is outlined in Chapter 3 and, from Zukoski, is corrected by dividing by a factor of two. DeZubay's experimental data were collected at a minimum-area static temperature of 550 °R +/- 30 °R; therefore, because DeZubay's experimental correlations do not include temperature effects, the comparison of U_{bo} predicted from LSENS to calculations from DeZubay's β-parameter is limited to predictions at comparable temperatures, namely 530 °R.

Figure 10 is a comparison of U_{bo} from LSENS predictions at T_2=530 °R to calculations from DeZubay's β-parameter corrected for two-dimensional flameholders. Note that φ=1.2 was the design point in the determination of V_R at the respective static pressures.

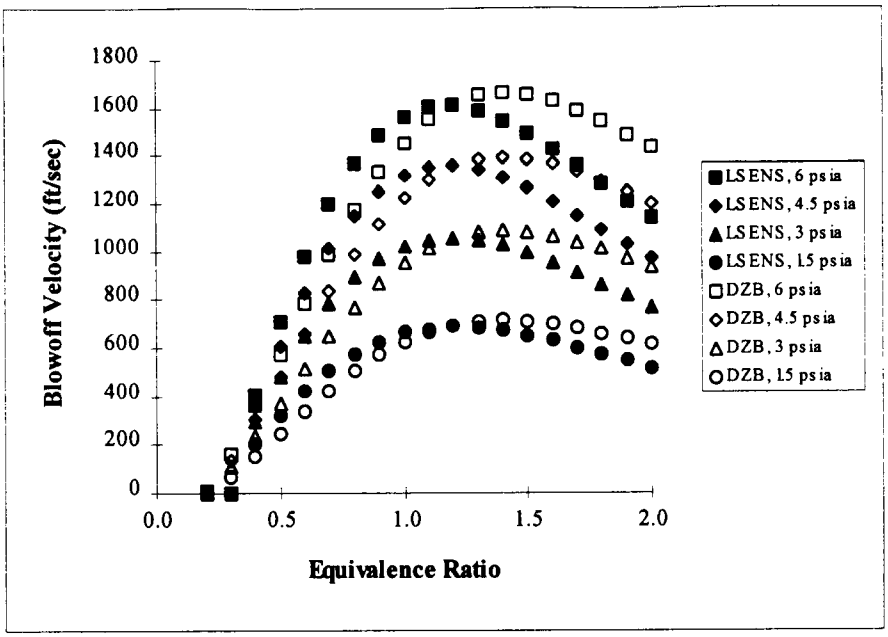

Figure 10: Comparison of Blowoff Velocity from LSENS Predictions at T_2=530 °R to Calculations from DeZubay's β-parameter

From Figure 10, the maximum value of U_{bo} from model predictions occurs at φ=1.2 for all pressures; whereas, the maximum blowoff velocity calculated from DeZubay's data occurs at φ=1.4. The discontinuity in the model predictions between $0.3<\varphi<0.4$ is discussed in the next section. The model predictions agree within 10% of DeZubay's corrected data for $1.0\leq\varphi\leq1.5$ over the entire pressure range. Also, the model predictions agree within 24% of DeZubay's corrected data for $\varphi\geq0.4$ at all pressures. For lean and rich mixtures at a given pressure, disagreement increased due to changes in wake dynamics which result from significant changes in the entrainment rates at lower and higher mixture densities; hence, significant changes in Reynolds number effects occur at lean and rich mixtures. At 1.5 psia, agreement between model predictions and DeZubay's corrected data was within 10% for $0.9\leq\varphi\leq1.6$ and within 16% for $\varphi\geq0.4$. At 6 psia, agreement between model predictions and DeZubay's corrected

data was within 10% for $1.0 \leq \varphi \leq 1.5$ and within 24% for $\varphi \geq 0.4$. At higher pressures, disagreement increases because Reynolds number effects were not included in the determination of V_R. For the well-stirred reactor model, the flow was considered inviscid; however, for real flows, viscosity, and therefore Reynolds number, has a significant influence on flame stability. For a flowing fluid, Reynolds number, Re, is defined as the ratio of inertia forces to viscous forces and, for a vee-gutter, is given by: $Re=(\rho U_{bo} w)/(g_c \mu)$. For the specified vee-gutter, the value of w is constant at 1.5 inches; U_{bo} is a function of φ; ρ is calculated from the equation of state and is also a function of φ. For gas flow problems, the coefficient of viscosity, μ, is a function of φ and temperature; however, at a given temperature, μ reduces solely to a function of φ. Figure 11 is a plot of blowoff Reynolds number calculated using the blowoff limits predicted by LSENS at T_2=530 °R.

To quantify the significance of Reynolds number effects, LSENS predictions of m_{max} were correlated to values of U_{bo} calculated from DeZubay's experimental data over the defined range of φ. For hydrogen-air mixtures over the isolated, vee-gutter flameholder, the values of e_t required to match m_{max} predicted by LSENS at T_2=530 °R to U_{bo} calculated from DeZubay's β-parameter was computed using Equation 5.1. Figure 12 is the plot of the required e_t as a function of φ.

Figure 12 demonstrates that Reynolds number effects play a significant role in flame stabilization on a bluff body. Matching LSENS predictions to DeZubay's corrected data requires entrainment of approximately 8.0% to 13.4% of the upstream flow through the projected area of the vee-gutter for $\varphi \geq 0.4$. This range of e_t roughly match the 8% to 12% predicted by Equation 2.4.

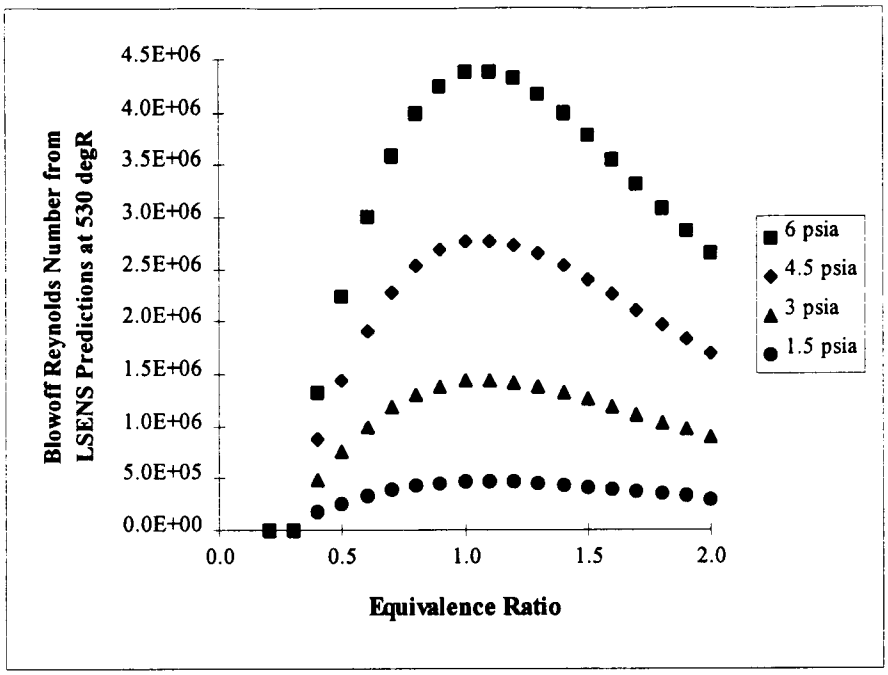

Figure 11: Blowoff Reynolds Number from LSENS Predictions at T_2=530 °R

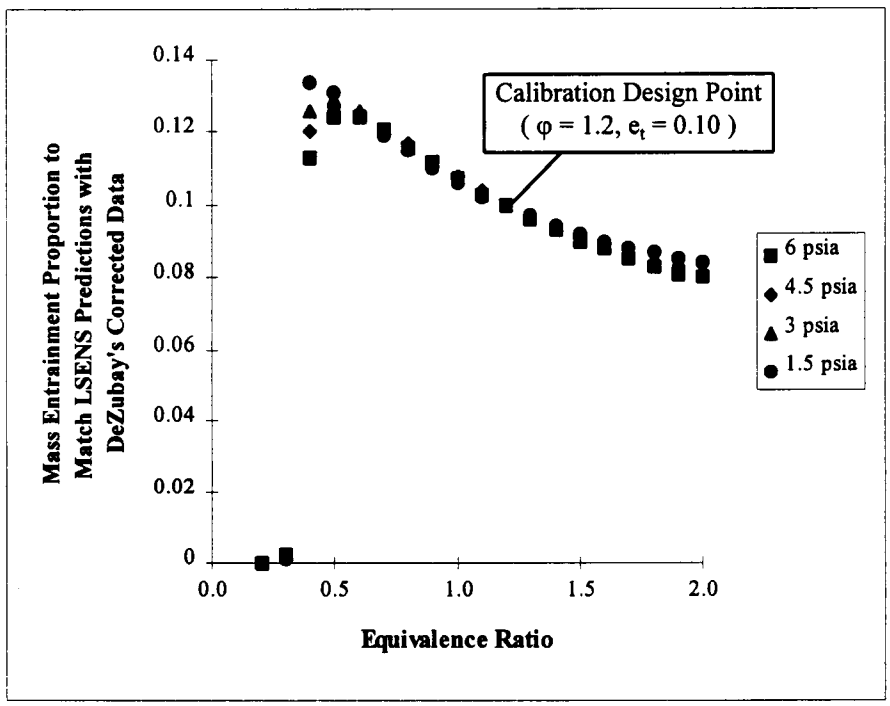

Figure 12: Entrainment Proportion Required to Match LSENS Predictions at T_2=530 °R to Blowoff Velocities from DeZubay's Corrected Data

For $\varphi \leq 0.3$, e_t is effectively zero due to the discontinuity in the model predictions; however, in reality, e_t remains non-zero even though blowoff has occurred.

PARAMETRIC STUDY OF PREDICTED FLAME BLOWOFF LIMITS

The author conducted a parametric study of U_{bo} predicted by the well-stirred reactor model to analyze the effects of flow conditions on flame stability. As a function of equivalence ratio, blowoff velocities were calculated using Equation 5.1. For the range of static pressures, Figure 13 contains plots of U_{bo} for hydrogen-air mixtures over the isolated vee-gutter with T_2=530 °R.

From Figure 13, U_{bo} decreases for decreasing static pressure at a given temperature. As a result, flame stability is questionable at pressures near 1 psia. At higher pressures, flame stability is a concern for $\varphi \leq 0.7$ and $\varphi \geq 1.9$. Outside of

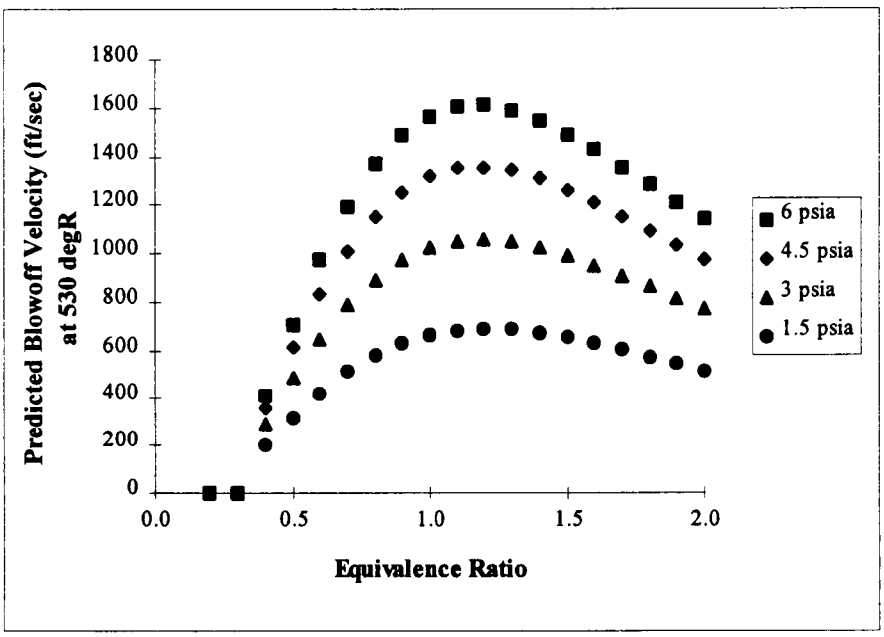

Figure 13: Blowoff Velocities for Hydrogen-Air Mixtures over the Isolated Vee-Gutter with T_2=530 °R

these limits, the flow velocity exceeds the critical Mach number of 0.46 for 30% geometric blockage produced by the given vee-gutter. Also in Figure 13, the discontinuity in the data between $0.3<\varphi<0.4$ results from the chemical reaction mechanism at small values of φ. At low pressure and temperature, the chemical induction time is relatively large and small values of φ cannot sustain the chemical kinetics. A more sophisticated set of chemical kinetics may result in uniform, monotonic behavior for the entire range of φ at low pressures and temperatures.

Figure 14 and Figure 15 contain plots of U_{bo} for hydrogen-air mixtures over the selected vee-gutter configuration with T_2=730 °R and T_2=930 °R, respectively.

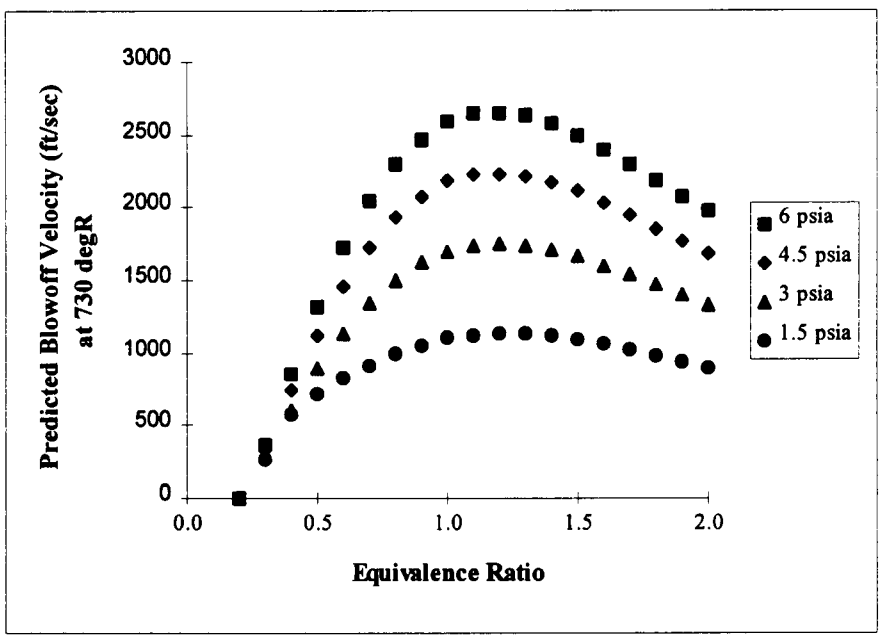

Figure 14: Blowoff Velocities for Hydrogen-Air Mixtures over the Isolated Vee-Gutter with T_2=730 °R

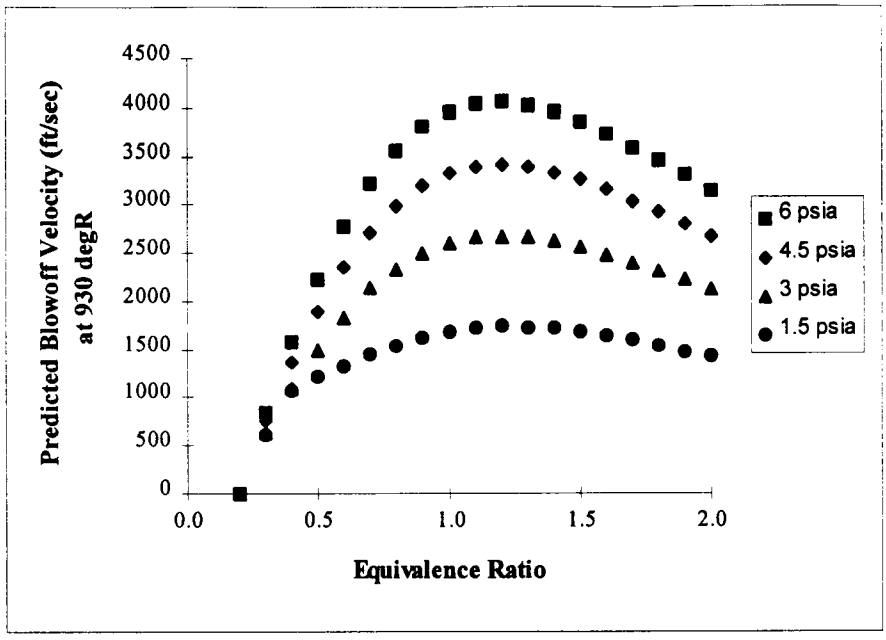

Figure 15: Blowoff Velocities for Hydrogen-Air Mixtures over the Isolated Vee-Gutter with T_2=930 °R

From Figures 14 and 15, U_{bo} increases for increasing static temperature at a given pressure as compared to Figure 13; therefore, flame stability is a concern at low temperatures. At higher temperatures ($T_2 \geq 730$ °R), flame stability is a concern for $\varphi \leq 0.5$. Outside of these limits, the flow velocity exceeds the critical Mach number of 0.46 for 30% geometric blockage produced by the given vee-gutter. In Figure 13, a discontinuity in the data occurs between $0.3<\varphi<0.4$ at T_2=530 °R; however, the discontinuity does not occur in Figures 14 and 15. Chemical induction time decreases with increasing temperature; therefore, at higher temperatures, the chemical induction time is sufficiently small to sustain combustion even at low pressures.

CHAPTER 6

CONCLUSIONS

The well-stirred reactor model of the recirculation zone of an isolated vee-gutter provides preliminary predictions of flame blowoff limits for premixed, turbulent hydrogen-air mixtures. Implementation of the model depends on specification of the mass proportion entrained into the recirculation zone and the effective volume of the recirculation zone. The mass proportion entrained into the recirculation zone was held constant at 10% of the upstream flow through the projected, frontal area of the vee-gutter for the defined range of static pressures. As a function of static pressure, the volume of the recirculation zone per unit span of the flameholder was calculated using Baxter and Lefebvre's correlation and DeZubay's corrected experimental data.

The model predictions at T_2=530 °R were compared to calculations from DeZubay's β-parameter corrected for two-dimensional flameholders. A discontinuity occurs in the model blowoff predictions between $0.3 \leq \varphi \leq 0.4$ and is a result of insufficient chemical induction times at extremely lean mixtures. The maximum U_{bo} occurs at φ=1.4 in DeZubay's experimental data and at φ=1.2 in the model predictions. The model predictions agree within 10% of DeZubay's corrected data for $1.0 \leq \varphi \leq 1.5$ over the entire pressure range. Also, for $\varphi \geq 0.4$, the model predictions agree with DeZubay's corrected data within 16% at 1.5 psia and within 24% at 6 psia. For lean and rich mixtures and for increasing pressures, disagreement increased presumably due to changes in wake dynamics which result from significant changes in Reynolds number. As previously demonstrated, Reynolds number effects on flame stability are significant. These effects,

however, are dependent on the flameholder configuration and must be empirically determined.

For various pressures and $\varphi \geq 0.4$, calculations of e_t based on matching LSENS predictions to DeZubay's corrected data requires entrainment of approximately 8.0% to 13.4% of the upstream flow through the projected frontal area of the vee-gutter. This range of e_t roughly matches the range calculated from Baxter and Lefebvre's correlation for vee-gutters. In general, e_t appears to increase as Reynolds number based on blowoff velocity decreases. Blowoff is affected by temperature as well as pressure; therefore, DeZubay's correlations are not sufficient for prediction of blowoff over vee-gutter flameholders for the range of static temperatures expected in test facility exhaust systems.

The parametric study of the LSENS predictions showed that flame blowoff for hydrogen-air mixtures over the selected vee-gutter configuration is a concern at low pressures and temperatures, especially for lean and rich mixtures

Flame stability is questionable at pressures on the order of 1 psia and at temperatures less than 730 ^{o}R. At higher pressures, flame stability is a concern for $\varphi \leq 0.7$ and $\varphi \geq 1.9$. Also, for higher temperatures, flame stability is a concern for $\varphi \leq 0.5$. For conditions outside of these limits, the blowoff velocities predicted by the well-stirred reactor model exceed the critical Mach number for the selected geometric configuration; therefore, due to aerodynamic blockage, the ducted, freestream flow will choke before blowoff occurs.

The discontinuities in the model predictions between $0.3 \leq \varphi \leq 0.4$ result from the complexity of the chemical kinetics at small values of φ. At low pressure and temperature, the chemical induction time is relatively large, and small values of φ cannot sustain the chemical kinetics. The discontinuity does not occur in the data for T_2=730 ^{o}R or T_2=930 ^{o}R. Chemical induction time decreases with increasing temperature; therefore,

at higher temperatures, the chemical induction time is sufficiently small to sustain combustion even at low pressures. A more sophisticated set of chemical kinetics may produce continuity for the entire range of φ at low pressures and temperatures.

For hydrogen-air mixtures over the selected vee-gutter, the well-stirred reactor model herein developed is limited by insufficient experimental data. Experimental or rigorous analytical determination of e_t and V_R for the representative vee-gutter configuration may improve the accuracy of the model. To further investigate the model's potential, the model can be applied to other fuels and/or flow geometries. The model predictions can then be compared to the existing experimental data concerning those fuels and flow geometries. Without precise experimental evidence, however, the well-stirred reactor model, as developed and applied in this study, provides a useful preliminary survey of the flame blowoff limits for premixed, turbulent hydrogen-air mixtures.

LIST OF REFERENCES

LIST OF REFERENCES

[1] S. E. Stephens, J. L. Jordan and R. J. Schulz, "Hydrogen-Rich Exhaust Gas Handing Studies," *Journal of Propulsion and Power*, Vol. 7, No. 2, March-April 1991, pp. 196-206.

[2] G. Garrard and C. Bartlett, "Hydrogen Exhaust Gas Disposition by Afterburning", AIAA-91-5075, AIAA Third International Aerospace Planes Conference, Orlando, FL, December 3-5, 1991.

[3] I. L. Drell and F. E. Belles "Survey of Hydrogen Combustion Properties," NACA Report 1383, NASA Lewis Flight Propulsion Laboratory, Cleveland, OH, 1958.

[4] D. R. Ballal and A. H. Lefebvre, "Weak Extinction Limits of Turbulent Flowing Mixtures," *Journal of Engineering for Power*, Vol. 101, No. 3, July 1979, pp. 343-348.

[5] T. W. Davies and J. M. Beer, "Flow in the Wake of Bluff-Body Flame Stabilizers," 13th Symposium (International) on Combustion, The Combustion Institute, Pittsburgh, 1971, pp. 631-638.

[6] A. H. Lefebvre, et al, "Factors Affecting Fresh Mixture Entrainment in Bluff-Body Stabilized Flames," 10th Symposium (International) on Combustion, The Combustion Institute, Pittsburgh, September 1966, pp. 231-239.

[7] G. Winterfeld, "On Processes of Turbulent Exchange Behind Flame Holders," 10th Symposium (International) on Combustion, The Combustion Institute, Pittsburgh, 1965, pp. 1265-1275.

[8] T. Carmody, "Establishment of the Wake Behind a Disk," *ASME Journal of Basic Engineering*, Vol. 86, No. 4, Ser D, December 1964, pp. 869-882.

[9] E. A. DeZubay, "Characteristics of Disk-Controlled Flame," *Aerodigest*, Vol. 61, No. 1, July 1950.

[10] E. A. DeZubay, "A Study of Flame Stability Based on Reaction Rate Theory," ASME Paper 54-SA-27, Presented at the Semi-Annual Meeting, Pittsburgh, PA, June 20-24, 1954.

[11] K. V. L. Rao and A. H. Lefebvre, "Flame Blowoff Studies Using Large-Scale Flameholders," *Journal of Engineering for Power*, Vol. 104, October 1982, pp. 853-857.

[12] M. R. Baxter and A. H. Lefebvre, "Weak Extinction Limits of Large Scale Flameholders," ASME-91-GT-234, Presented at the International Gas Turbine and Aeroengine Congress and Exposition, Orlando, FL, June 3-6, 1991.

[13] R. M. Stwalley, III and A. H. Lefebvre, "Flame Stabilization Using Large Scale Flame Holders of Irregular Shape," *Journal of Propulsion*, Vol. 4, No. 1, January 1988, pp. 4-13.

[14] N. K. Rizk and A. H. Lefebvre, "The Relationship Between Flame Stability and Drag of Bluff-Body Flameholders," *AIAA Journal of Propulsion*, Vol. 2, No. 4, July-August 1986, pp. 361-365.

[15] D. A. Bittker and V. J. Scullin, "GCKP84 - General Chemical Kinetics Code for Gas-Phase Flow and Batch Processes Including Heat Transfer Effects," NASA Technical Paper 2320, Lewis Research Center, Cleveland, OH, September 1984.

[16] K. Radhakrishnan and D. A. Bittker, "LSENS, A General Chemical Kinetics and Sensitivity Analysis Code for Gas-Phase Reactions: User's Guide," NASA Technical Memorandum 105851, Lewis Research Center, Cleveland, OH, January 1993.

[17] E. E. Zukoski, "Afterburners," Chapter 21 - The Aerodynamics of Gas Turbine Engines, edited by G. C. Oates, AFAPL-TR-78-52, July 1958.

[18] R. I. Ozawa, "Survey of Basic Data on Flame Stabilization and Propagation for High Speed Combustion Systems," Technical Report AFAPL-TR-70-81, The Marquardt Company, Wright-Patterson Air Force Base, OH, January 1971.

[19] J. P. Longwell, E. E. Frost and M. A. Weiss, "Flame Stability in Bluff Body Recirculation Zones," *Industrial and Engineering Chemistry*, Vol. 45, No. 8, 1953, pp. 1629-1633.

[20] E. E. Zukoski and F. E. Marble, "The Role of Wake Transition in the Process of Flame Stabilization on Bluff Bodies," AGARD Combustion Researches and Reviews, London: Butterworths Scientific Publishers, 1955, pp. 167-180.

[21] D. W. Roberds, et al, "Measurements of Residence Time, Air Entrainment Rate and Base Pressure in the Near Wake of a Cylindrical Body in Subsonic Flow," *AIAA Journal*, Vol. 27, No. 11, November 1989, pp. 1524-1529.

[22] J. P. Longwell and M. A. Weiss, *Industrial and Engineering Chemistry*, Vol. 47, 1955, pp. 1634.

[23] A. Jones and A. Prothero, "The Solution of the Steady State Equations for an Adiabatic Stirred Reactor," *Combustion and Flame*, Vol. 2, No. 5, October 1968, pp. 457-464.

[24] J. D. Anderson, Jr., Modern Compressible Flow with Historical Perspective - Second Edition, McGraw-Hill Publishing Company, New York, 1990, pp. 618-622.

[25] R. G. Abdel-Gayed, et. al., "Turbulent Burning Velocities: A General Correlation in Terms of Straining Rates," Proceedings of the Royal Society of London, A414, 1987, pp. 389-413.

[26] F. H. Wright, "Bluff Body Flame Stabilization: Blockage Effects," *Combustion and Flame*, Vol. 3, p. 319, 1959.

[27] D. A. Bittker, Phone Conversation with the Author, NASA Lewis Research Center, Cleveland, OH, January 27, 1994.

APPENDICES

APPENDIX A

SAMPLE LSENS INPUT DATA FILE

```
LSENS   HYDROGEN-AIR: WELL-STIRRED REACTOR MODEL
  O      + H2O   = OH     + OH              6.8E+13  0.      18365.
  H      + O2    = OH     + O               1.89E+14 0.      16400.
  O      + H2    = OH     + H               4.20E+14 0.      13750.
  H      + HO2   = H2     + O2              7.28E+13 0.      2126.
  O      + HO2   = OH     + O2              5.0E+13  0.      1000.
  HO2    + OH    = H2O    + O2              8.0E+12  0.      0.
  H      + HO2   = 2.0 OH                   1.34E+14 0.      1070.
  H2     + HO2   = H2O2   + H               7.91E+13 0.      25000.
  OH     + H2O2  = H2O    + HO2             6.1E+12  0.      1430.
  HO2    + HO2   = H2O2   + O2              1.8E+12  0.      0.
  H      + H2O2  = OH     + H2O             7.8E+11  0.      0.
  M      + H2O2  = 2.0 OH                   1.44E+17 0.      45510.
  THIRDBODY
H2      2.30  O2      .78   H2O      6.0   H2O2     6.6
END
  H2     + OH    = H2O    + H               4.74E+13 0.      6098.
  H      + O2    = HO2    + M               1.46E+15 0.      -1000.
  THIRDBODY
O2      1.30  N2      1.3   H2O      21.3  H2       3.0
END
  M      + H2O   = H      + OH              1.30E+15 0.      105140.
  THIRDBODY
H2      4.00  O2      1.5   H2O      20.0  N2       1.5
END
  H      + O     = OH     + M               7.1E+18  -1.     0.
  M      + H2    = H      + H               2.2E+14  0.      96000.
  THIRDBODY
H2      4.10  O2      2.0   H2O      15.0  N2       2.0
END
  M      + O2    = O      + O               1.80E+18 -1.     118020.
  HO2    + NO    = NO2    + OH              2.09E+12  0.     -477.
  O      + NO2   = NO     + O2              1.0E+13   0.     596.
  NO     + O     = NO2    + M               5.62E+15 0.      -1160.
  NO2    + H     = NO     + OH              3.47E+14 0.      1470.
  NO     + O     = N      + O2              3.8E+9  1.       41370.
  O      + N2    = NO     + N               1.8E+14  0.      76250.
  NO     + H     = N      + OH              2.63E+14 0.      50410.
  M      + N2O   = N2     + O               6.92E+23 -2.5    65000.
  O      + N2O   = N2     + O2              1.0E+14  0.      28020.
  O      + N2O   = 2.0 NO                   6.92E+13 0.      26630.
  N      + NO2   = 2.0 NO                   4.0E+12  0.      0.
  N2O    + H     = N2     + OH              7.59E+13 0.      15100.
  NO2    + H2    = HNO2   + H               2.4E+13  0.      29000.
  OH     + NO2   = HNO3   + M               3.0E+15  0.      -3800.
  THIRDBODY
O2      0.70  H2      1.4   END
  OH     + NO    = HNO2   + M               5.6E+15  0.      -1700.
  HNO    + H     = H2     + NO              5.0E+12  0.      0.
  H      + NO    = HNO    + M               5.4E+15  0.      -600.
  HNO    + OH    = H2O    + NO              3.6E+13  0.      0.
```

```
CO2     AR
TIME    PRESSURE FPS     FPS     H2
&PROB
                PRINT=0.0005,0.001,0.0025,0.005,0.0075,0.01,0.05,0.10
                HTRAN =.FALSE.,
                WELSTR=.TRUE.,
                CONC=.FALSE.,
                PCON=.TRUE.
&END
&WSPROB
                DOTMAX=5.000,
                DELMD=0.0001,
                MPR=1.0,
                VOLUME=0.00303
                WSRHTR=.FALSE.,
&END
&START
                P=432.0,
                T=530.0,
                MDOT=0.1050,
                ERATIO=1.0,
                SCC=0.0,
                SCH=2.0,
                SCOX=0.0,
                TIME=0.0,
&END
END
 &SOLVER
                EMAX=1.0E-3
                ATOLSP=1.0E-11
&END
FINIS
```

APPENDIX B

AERODYNAMIC WIDTH OF THE RECIRCULATION ZONE BEHIND THE SELECTED VEE-GUTTER

For the selected geometric configuration of vee-gutter and flow field (see Figure 4, p. 17):

$w = 1.5$ in.

$\theta = 30^o$

$W = 5$ in.

Geometric Blockage of Flameholder: $B_G = A_f / A_1 = w / W = 1.5$ in./ 5 in.$= 0.3$

From Baxter and Lefebvre,[12]

Drag Coefficient: $C_D = (\sin \theta/2)^{1/4} = (\sin 30^o/2)^{1/4} = 0.71$ (B.1)

Aerodynamic Blockage: $B_A = (1-B_G)^2 / [(1-B_G)^2 + 3.7C_DB_G]$ (B.2)

$B_A = 0.38$

However, $B_A = w_A/W$, where w_A is the aerodynamic width of the recirculation zone behind the vee-gutter flameholder; therefore,

$$w_A = B_A W = 0.38(5 \text{ in}) = 1.9 \text{ in.}$$

APPENDIX C

EQUIVALENT DISK DIAMETER FOR SAME AERODYNAMIC BLOCKAGE AS ONE-FOOT SPAN OF VEE-GUTTER

For the 1-ft span of vee-gutter: $B_A = (w_A\ S) / (W\ S) = 0.38$

$w_A = 1.9$ in.

From DeZubay:[12]

aerodynamic diameter = 1.8 d

For equivalent aerodynamic blockage:

$$B_A = (w_A\ S) / (W\ S) = \pi\ (1.8\ d)^2 / (W\ S)$$

Therefore, $d = \{[(w_A\ S) / \pi]^{1/2}\} / 1.8$

$d = \{[(1.9\text{ in.})(12\text{ in.}) / \pi]^{1/2}\} / 1.8$

$d = 1.5$ in.

APPENDIX D

SAMPLE LSENS OUTPUT DATA FILE FOR APPARENT BLOWOUT CONDITION

***** PRECEDING DATA DELETED FOR SPACE *****

** ASSIGNED VARIABLE PROFILE **
WELL - STIRRED REACTOR CASE
VOLUME OF REACTOR = 8.51000E-03 FT**3
MASS FLOW RATE TO START ITERATION = 2.75000E-01 LBM/S

ASSIGNED MASS FLOW RATE PROBLEM:
MASS FLOW RATE INCREMENT = 1.00000E-03 LB/S
MAXIMUM MASS FLOW RATE = 5.00000E+00 LB/S
AIR - FUEL COMBUSTION, EQUIVALENCE RATIO = 1.0000
OXYGEN FRACTION IN AIR = 0.2095
NUMBER OF REACTING SPECIES: 16
NUMBER OF INERT SPECIES: 2

** INITIAL CONDITIONS **
TIME 0.00000E+00 SEC
AREA 0.00000E+00 SQ FT
AXIAL POSITION 0.00000E+00 FT

FLOW PROPERTIES		INTEGRATION INDICATORS	
PRESSURE (LB/FT**2)	4.32000E+02	STEPS FROM LAST PRINT	0
VELOCITY (FT/SEC)	0.00000E+00	AVERAGE STEP SIZE	0.00000E+00
DENSITY (LB/FT**3)	1.10808E-02	METHOD ORDER	0
TEMPERATURE (DEG R)	530.00		
MASS FLOW RATE (LB/SEC)	2.75000E-01	TOTAL NUMBER OF STEPS	0
ENTROPY (BTU/LB/DEG R)	2.23549E+00	FUNCT EVALUATIONS	0
MACH NUMBER	0.00000E+00	JACOBIAN EVALUATIONS	0
GAMMA	1.40156E+00		
ENTHALPY (BTU/LB)	-3.87912E+00		
SP. HEAT (CP) (BTU/LB/DEG R)	3.30167E-01		

***** INTERMEDIATE DATA DELETED FOR SPACE *****

MIXTURE MOLECULAR WEIGHT 21.00704
TOTAL ENERGY EXCHANGE RATE 6.80953E-28
MASS FRACTION SUM 1.00000000
(BTU-FT**3/LB**2/SEC)

**EQUILIBRIUM CONDITIONS **

TIME 0.00000E+00 SEC
AREA 0.00000E+00 SQ FT
AXIAL POSITION 0.00000E+00 FT

FLOW PROPERTIES		INTEGRATION INDICATORS	
PRESSURE (LB/FT**2)	4.32000E+02	STEPS FROM LAST PRINT	0
VELOCITY (FT/SEC)	0.00000E+00	AVERAGE STEP SIZE	0.00000E+00
DENSITY (LB/FT**3)	1.62150E-03	METHOD ORDER	0
TEMPERATURE (DEG R)	4183.74		
MASS FLOW RATE (LB/SEC)	2.75000E-01	TOTAL NUMBER OF STEPS	0
ENTROPY (BTU/LB/DEG R)	2.76488E+00	FUNCT EVALUATIONS	0
MACH NUMBER	0.00000E+00	JACOBIAN EVALUATIONS	0
GAMMA	1.25066E+00		
ENTHALPY (BTU/LB)	-3.87887E+00		
SP. HEAT (CP) (BTU/LB/DEG R)	4.08596E-01		

***** INTERMEDIATE DATA DELETED FOR SPACE *****

MIXTURE MOLECULAR WEIGHT 24.26602
TOTAL ENERGY EXCHANGE RATE 2.52388E+05
MASS FRACTION SUM 1.00000006
(BTU-FT**3/LB**2/SEC)

INITIAL ESTIMATES(SIGMAS) AT TEMPERATURE = 2324.30 K

O	4.26102E-05
H2O	1.29698E-02
OH	3.75868E-04
H	1.40878E-04
O2	2.79059E-04
H2	8.27940E-04
HO2	5.69464E-08
H2O2	2.22498E-09
NO	1.09605E-04
NO2	9.78718E-09
N	3.66026E-09
N2	2.61413E-02
N2O	2.48715E-09
HNO2	1.00000E-10
HNO3	1.00000E-10
HNO	2.69873E-09
CO2	1.00642E-05
AR	3.12658E-04

WELLSTIRRED REACTOR CALCULATION....
LSENS HYDROGEN-AIR: WELL-STIRRED REACTOR MODEL

		INITIAL STATE	FINAL STATE	FINAL/INITIAL RATIO
PRESSURE	LB/FT**2	432.000	432.000	1.00000
TEMP.	DEG R	530.000	2080.10	3.92472
ENTROPY	BTU/LB/R	2.23549	2.65868	1.18931
DENSITY	LB/FT**3	1.10808E-02	2.97338E-03	0.26834
ENTHALPY	BTU/LB	-3.87912	-3.87922	1.00002
SP. HEAT (CP)	BTU/LB/R	3.30167E-01	3.68354E-01	1.11566
MOL. WT. OF MIXT		21.0070	22.1234	
GAMMA		1.4016	1.3225	

SPECIES	MOLE FRACT	MASS FRACT	MOLE FRACT	MASS FRACT
O	0.00000E+00	0.00000E+00	5.64017E-03	4.07890E-03
H2O	0.00000E+00	0.00000E+00	1.76929E-01	1.44074E-01
OH	0.00000E+00	0.00000E+00	3.15060E-03	2.42201E-03
H	0.00000E+00	0.00000E+00	6.50122E-02	2.96203E-03
O2	1.47639E-01	2.24890E-01	6.26121E-02	9.05606E-02
H2	2.95278E-01	2.83344E-02	9.99535E-02	9.10737E-03
HO2	0.00000E+00	0.00000E+00	1.30972E-05	1.95401E-05
H2O2	0.00000E+00	0.00000E+00	3.17469E-07	4.88107E-07
NO	0.00000E+00	0.00000E+00	1.80554E-07	2.44886E-07
NO2	0.00000E+00	0.00000E+00	4.59419E-08	9.55358E-08
N	0.00000E+00	0.00000E+00	2.21234E-09	1.40067E-09
N2	5.50303E-01	7.33842E-01	5.79548E-01	7.33842E-01
N2O	0.00000E+00	0.00000E+00	2.21234E-09	4.40128E-09
HNO2	0.00000E+00	0.00000E+00	1.24694E-06	2.64981E-06
HNO3	0.00000E+00	0.00000E+00	2.21234E-09	6.30128E-09
HNO	0.00000E+00	0.00000E+00	2.21234E-09	3.10140E-09
CO2	2.11419E-04	4.42924E-04	2.22655E-04	4.42924E-04
AR	6.56802E-03	1.24901E-02	6.91707E-03	1.24901E-02

VOLUME 0.850995E-02 FT**3 MASS FLO 0.275000 LB/SEC
MDOT/VOLUME = 32.31513 RESIDENCE TIME = 0.0920 MSEC ITERATIONS = 12

***** INTERMEDIATE ITERATIONS DELETED FOR SPACE *****

WELLSTIRRED REACTOR CALCULATION....
LSENS HYDROGEN-AIR: WELL-STIRRED REACTOR MODEL

	INITIAL STATE	FINAL STATE	FINAL/INITIAL RATIO
PRESSURE LB/FT**2	432.000	432.000	1.00000
TEMP. DEG R	530.000	2036.82	3.84306
ENTROPY BTU/LB/R	2.23549	2.65303	1.18678
DENSITY LB/FT**3	1.10808E-02	3.03212E-03	0.27364
ENTHALPY BTU/LB	-3.87912	-3.87907	0.999988
SP. HEAT (CP) BTU/LB/R	3.30167E-01	3.67100E-01	1.11186
MOL. WT. OF MIXT	21.0070	22.0911	
GAMMA	1.4016	1.3246	

SPECIES	MOLE FRACT	MASS FRACT	MOLE FRACT	MASS FRACT
O	0.00000E+00	0.00000E+00	4.91344E-03	3.55854E-03
H2O	0.00000E+00	0.00000E+00	1.68783E-01	1.37642E-01
OH	0.00000E+00	0.00000E+00	2.69963E-03	2.07837E-03
H	0.00000E+00	0.00000E+00	6.06793E-02	2.76867E-03
O2	1.47639E-01	2.24890E-01	6.70450E-02	9.71144E-02
H2	2.95278E-01	2.83344E-02	1.10035E-01	1.00407E-02
HO2	0.00000E+00	0.00000E+00	1.42245E-05	2.12531E-05
H2O2	0.00000E+00	0.00000E+00	2.74951E-07	4.23355E-07
NO	0.00000E+00	0.00000E+00	2.20911E-09	3.00061E-09
NO2	0.00000E+00	0.00000E+00	2.20911E-09	4.60055E-09
N	0.00000E+00	0.00000E+00	2.20911E-09	1.40067E-09
N2	5.50303E-01	7.33842E-01	5.78700E-01	7.33842E-01
N2O	0.00000E+00	0.00000E+00	2.20911E-09	4.40128E-09
HNO2	0.00000E+00	0.00000E+00	2.20911E-09	4.70134E-09
HNO3	0.00000E+00	0.00000E+00	2.20911E-09	6.30128E-09
HNO	0.00000E+00	0.00000E+00	2.20911E-09	3.10140E-09
CO2	2.11419E-04	4.42924E-04	2.22329E-04	4.42924E-04
AR	6.56802E-03	1.24901E-02	6.90695E-03	1.24901E-02

VOLUME 0.850995E-02 FT**3 MASS FLO 0.281000 LB/SEC
MDOT/VOLUME = 33.02018 RESIDENCE TIME = 0.0918 MSEC ITERATIONS = 3

0(WSR) *** FOR CONV. NO. 8, CONVERGED TEMP. (AFTER 12 ITERATIONS)
IS NOT MUCH GREATER THAN THE INLET TEMP. - APPARENT BLOWOUT ***
MASS FLOW RATE = 2.54919E+02 G/S,
TEMPERATURE = 2.94435E+02 K,
INLET TEMPERATURE = 2.94444E+02 K

WSR SOLUTIONABANDONED

0(LSENS) A FATAL ERROR HAS OCCURRED - CASE TERMINATED

APPENDIX E

SAMPLE LSENS OUTPUT DATA FILE FOR NON-CONVERGENCE CONDITION

***** PRECEDING DATA DELETED FOR SPACE *****

** ASSIGNED VARIABLE PROFILE **
WELL - STIRRED REACTOR CASE
VOLUME OF REACTOR = 8.51000E-03 FT**3
MASS FLOW RATE TO START ITERATION = 1.95000E-01 LBM/S

ASSIGNED MASS FLOW RATE PROBLEM:
MASS FLOW RATE INCREMENT = 2.00000E-04 LB/S
MAXIMUM MASS FLOW RATE = 5.00000E+00 LB/S
AIR - FUEL COMBUSTION, EQUIVALENCE RATIO = 0.6000
OXYGEN FRACTION IN AIR = 0.2095
NUMBER OF REACTING SPECIES: 16
NUMBER OF INERT SPECIES: 2

** INITIAL CONDITIONS **
TIME 0.00000E+00 SEC
AREA 0.00000E+00 SQ FT
AXIAL POSITION 0.00000E+00 FT

FLOW PROPERTIES		NTEGRATION INDICATORS	
PRESSURE (LB/FT**2)	4.32000E+02	STEPS FROM LAST PRINT	0
VELOCITY (FT/SEC)	0.00000E+00	AVERAGE STEP SIZE	0.00000E+00
DENSITY (LB/FT**3)	1.24225E-02	METHOD ORDER	0
TEMPERATURE (DEG R)	530.00		
MASS FLOW RATE (LB/SEC)	1.95000E-01	TOTAL NUMBER OF STEPS	0
ENTROPY (BTU/LB/DEG R)	2.05044E+00	FUNCT EVALUATIONS	0
MACH NUMBER	0.00000E+00	JACOBIAN EVALUATIONS	0
GAMMA	1.40105E+00		
ENTHALPY (BTU/LB)	-3.66799E+00		
SP. HEAT (CP) (BTU/LB/DEG R)	2.94771E-01		

MIXTURE MOLECULAR WEIGHT 23.55054
TOTAL ENERGY EXCHANGE RATE 4.17993E-28
MASS FRACTION SUM 1.00000000
(BTU-FT**3/LB**2/SEC)

**EQUILIBRIUM CONDITIONS **

TIME 0.00000E+00 SEC
AREA 0.00000E+00 SQ FT
AXIAL POSITION 0.00000E+00 FT

FLOW PROPERTIES		INTEGRATION INDICATORS	
PRESSURE (LB/FT**2)	4.32000E+02	STEPS FROM LAST PRINT	0
VELOCITY (FT/SEC)	0.00000E+00	AVERAGE STEP SIZE	0.00000E+00
DENSITY (LB/FT**3)	2.21786E-03	METHOD ORDER	0
TEMPERATURE (DEG R)	3298.46		
MASS FLOW RATE (LB/SEC)	1.95000E-01	TOTAL NUMBER OF STEPS	0
ENTROPY (BTU/LB/DEG R)	2.48802E+00	FUNCT EVALUATIONS	0
MACH NUMBER	0.00000E+00	JACOBIAN EVALUATIONS	0
GAMMA	1.27217E+00		
ENTHALPY (BTU/LB)	-3.66792E+00		
SP. HEAT (CP) (BTU/LB/DEG R)	3.54952E-01		

MIXTURE MOLECULAR WEIGHT 26.16756
TOTAL ENERGY EXCHANGE RATE 5.68785E+04
MASS FRACTION SUM 1.00000004
(BTU-FT**3/LB**2/SEC)

INITIAL ESTIMATES(SIGMAS) AT TEMPERATURE = 1832.48 K

O	3.73143E-06
H2O	8.49732E-03
OH	5.55710E-05
H	4.50970E-07
O2	2.78137E-03
H2	5.02042E-06
HO2	4.72087E-08
H2O2	1.05556E-09
NO	9.77154E-05
NO2	6.18664E-08
N	1.00000E-10
N2	2.64475E-02
N2O	2.38681E-09
HNO2	9.34814E-10
HNO3	1.00000E-10
HNO	1.00000E-10
CO2	1.01796E-05
AR	3.16243E-04

WELLSTIRRED REACTOR CALCULATION....
LSENS HYDROGEN-AIR: WELL-STIRRED REACTOR MODEL

		INITIAL STATE	FINAL STATE	FINAL/INITIAL RATIO
PRESSURE	LB/FT**2	432.000	432.000	1.00000
TEMP.	DEG R	530.000	1973.19	3.72301
ENTROPY	BTU/LB/R	2.05044	2.40695	1.17387
DENSITY	LB/FT**3	1.24225E-02	3.50625E-03	0.28225
ENTHALPY	BTU/LB	-3.66799	-3.67450	1.00177
SP. HEAT (CP)	BTU/LB/R	2.94771E-01	3.28395E-01	1.11407
MOL. WT. OF MIXT		23.5505	24.7474	
GAMMA		1.4011	1.3237	

SPECIES	MOLE FRACT	MASS FRACT	MOLE FRACT	MASS FRACT
O	0.00000E+00	0.00000E+00	5.66622E-03	3.66326E-03
H2O	0.00000E+00	0.00000E+00	1.40676E-01	1.02407E-01
OH	0.00000E+00	0.00000E+00	2.70436E-03	1.85853E-03
H	0.00000E+00	0.00000E+00	3.33748E-02	1.35936E-03
O2	1.67413E-01	2.27468E-01	1.01378E-01	1.31083E-01
H2	2.00895E-01	1.71955E-02	5.23792E-02	4.26654E-03
HO2	0.00000E+00	0.00000E+00	1.93435E-05	2.57992E-05
H2O2	0.00000E+00	0.00000E+00	5.21784E-07	7.17177E-07
NO	0.00000E+00	0.00000E+00	2.47474E-09	3.00061E-09
NO2	0.00000E+00	0.00000E+00	2.47474E-09	4.60055E-09
N	0.00000E+00	0.00000E+00	2.47474E-09	1.40067E-09
N2	6.24005E-01	7.42255E-01	6.55718E-01	7.42255E-01
N2O	0.00000E+00	0.00000E+00	2.47474E-09	4.40128E-09
HNO2	0.00000E+00	0.00000E+00	2.47474E-09	4.70134E-09
HNO3	0.00000E+00	0.00000E+00	5.36358E-06	1.36569E-05
HNO	0.00000E+00	0.00000E+00	2.47474E-09	3.10140E-09
CO2	2.39735E-04	4.48001E-04	2.51919E-04	4.48001E-04
AR	7.44768E-03	1.26333E-02	7.82619E-03	1.26333E-02

0 VOLUME 0.850995E-02 FT**3 MASS FLO 0.195000 LB/SEC
0 MDOT/VOLUME = 22.91436 RESIDENCE TIME = 0.1530 MSEC ITERATIONS = 14

WELLSTIRRED REACTOR CALCULATION....
LSENS HYDROGEN-AIR: WELL-STIRRED REACTOR MODEL

		INITIAL STATE	FINAL STATE	FINAL/INITIAL RATIO
PRESSURE	LB/FT**2	432.000	432.000	1.00000
TEMP.	DEG R	530.000	1926.33	3.63458
ENTROPY	BTU/LB/R	2.05044	2.40120	1.17107
DENSITY	LB/FT**3	1.24225E-02	3.58549E-03	0.28863

ENTHALPY	BTU/LB	-3.66799	-3.66795	0.999990
SP. HEAT (CP)	BTU/LB/R	2.94771E-01	3.27181E-01	1.10995
MOL. WT. OF MIXT		23.5505	24.7057	
GAMMA		1.4011	1.3260	

SPECIES	MOLE FRACT	MASS FRACT	MOLE FRACT	MASS FRACT
O	0.00000E+00	0.00000E+00	4.76625E-03	3.08663E-03
H2O	0.00000E+00	0.00000E+00	1.33772E-01	9.75454E-02
OH	0.00000E+00	0.00000E+00	2.26947E-03	1.56230E-03
H	0.00000E+00	0.00000E+00	3.09301E-02	1.26192E-03
O2	1.67413E-01	2.27468E-01	1.05199E-01	1.36254E-01
H2	2.00895E-01	1.71955E-02	6.03665E-02	4.92546E-03
HO2	0.00000E+00	0.00000E+00	2.05572E-05	2.74644E-05
H2O2	0.00000E+00	0.00000E+00	4.46978E-07	6.15397E-07
NO	0.00000E+00	0.00000E+00	2.47057E-09	3.00061E-09
NO2	0.00000E+00	0.00000E+00	2.47057E-09	4.60055E-09
N	0.00000E+00	0.00000E+00	2.47057E-09	1.40067E-09
N2	6.24005E-01	7.42255E-01	6.54611E-01	7.42255E-01
N2O	0.00000E+00	0.00000E+00	2.47057E-09	4.40128E-09
HNO2	0.00000E+00	0.00000E+00	2.47057E-09	4.70134E-09
HNO3	0.00000E+00	0.00000E+00	2.47057E-09	6.30128E-09
HNO	0.00000E+00	0.00000E+00	2.47057E-09	3.10140E-09
CO2	2.39735E-04	4.48001E-04	2.51493E-04	4.48001E-04
AR	7.44768E-03	1.26333E-02	7.81298E-03	1.26333E-02

0 VOLUME 0.850995E-02 FT**3 MASS FLO 0.199800 LB/SEC
0 MDOT/VOLUME = 23.47841 RESIDENCE TIME = 0.1527 MSEC ITERATIONS = 3

0(WSR) *** 75 ITERATIONS DID NOT SATISFY CONVERGENCE REQUIREMENTS ***
MDOT = 9.07185E+01 G/S TEMPERATURE = 1.07678E+03 K
WSR SOLUTION ABANDONED

CURRENT TEMPERATURE ESTIMATE IS 1076.78 K
ITERATION 75 MDOT = 9.07185E+01 G/S

0(LSENS) A FATAL ERROR HAS OCCURRED - CASE TERMINATED

APPENDIX F

DERIVATION OF THE EQUATION FOR BLOWOFF VELOCITY FOR THE REPRESENTATIVE GEOMETRIC CONFIGURATION

For the selected vee-gutter configuration (see Figure 4, p. 15):

$A_1 = 20\ in^2$

$A_f = 6\ in^2$

$A_2 = 14\ in^2$

Geometric Blockage is defined as: $B_G = A_f / A_1$

From Roberds, et al,[12] the mass entrained behind the flameholder is some proportion, e_t, of the upstream mass flow through the projected area of the flameholder; therefore,

$$m_{ent} = e_t m_f \quad \Rightarrow \quad m_f = m_{ent}/e_t \tag{F.1}$$

Assuming ideal gas behavior ($P = \rho RT$) with $R = f(\varphi)$,

$$m_f = (P_1 U_1 A_f)/(RT_1) \text{ and } m_1 = (P_1 U_1 A_1)/(RT_1)$$

Combining these two equations $\Rightarrow$ $m_f = A_f m_1/A_1 = m_1 B_G$ (F.2)

From Continuity: $m_1 = m_2$ $\Rightarrow$ $m_f = m_2 B_G$ (F.3)

Also, $m_2 = (P_2 U_2 A_2)/(RT_2)$ (F.4)

Combining Equations F.1, F.3 and F.4 and solving for U_2:

$$U_2 = (m_{ent} RT_2)(e_t P_2 A_2 B_G)^{-1} \tag{F.5}$$

Let m_{ent} equal the maximum mass flow rate, m_{max}, for a predicted stable flame determined from LSENS well-stirred reactor solution. The values of m_{max} were determined assuming a unit span of 1 ft. The actual length of the flameholder exposed to is 4 inches; therefore, the mass entrained behind the given flameholder is one-third m_{max} predicted by LSENS. The equation for blowoff velocity then becomes:

$$U_{bo} = (m_{max} RT_2)(3 e_t P_2 A_2 B_G)^{-1} \tag{F.6}$$

VITA

Julie Ann Darnell was born in Greenup County, Kentucky on June 13, 1968. She attended Greysbranch Elementary and graduated from Greenup County High School in May, 1986. The following August she entered the Pre-Engineering Program at Georgetown College in Georgetown, Kentucky. In August, 1990, she transferred to Washington University in St. Louis, Missouri. In May, 1992, she received the Bachelor of Science in Engineering Arts with a minor in Mathematics from Georgetown College, graduating *Summa Cum Laude*. Also in May, she received the Bachelor of Science in Mechanical Engineering from Washington University in St. Louis. In August, 1992, she began graduate studies at the University of Tennessee Space Institute in Tullahoma, Tennessee. In August, 1995, she received the Master of Science in Mechanical Engineering.

Since September, 1994, she has been employed as a Test Engineer assigned to General Electric Aircraft Engines, Peebles Test Operation in Peebles, Ohio.